

## Chapter 4

### Results and Discussion

#### 4.1 Bone Ash Powder

##### 4.1.1 Ca/Pmole Ratio and Impurity of Bone Ash Powder.

Table 10 Ca/P mole ratio and impurities in bone ash powder, characterized by Mineral Assay and Service.

---

Characteristic	Bone Ash Powder
Ca/P mole ratio	1.65/1
Impurities	
Mg (%)	1.05
Fe (%)	< 0.01
Zn (ppm)	92
Cu (ppm)	2
Mn (ppm)	5

---

## Heavy Metals. (ppm)

Cd	< 0.5
Pd	< 5
Hg	< 1
As	< 0.5
Ni	2

---

Table 10 showed Ca/P mole ratio and amount of impurities, analyzed by Department of Science and Service and, Mineral Assay and Service Company, respectively.

The average mole ratio of Ca/P in the bone ash was found to be 1.65 which was less than 1.67 of the stoichiometric hydroxyapatite. Therefore the bone ash used was a deficient hydroxyapatite of which main impurities were Mg, Fe and appreciable trace of Zn.

#### 4.1.2 Phase Present of Bone Ash Powder

XRD pattern of bone ash powder (calcined at 700°C.3 hours) . in Fig.13 showed d- spacing of 2.81( $2\theta=31.8^\circ$ ), 2.78( $2\theta=32.1^\circ$ ) and 2.72 ( $2\theta= 32.1^\circ$ ) which agreed with the powder diffraction card of hydroxyapatite (OHAp; $\text{Ca}_5(\text{PO}_4)_3(\text{OH})$ ) and there was no second phase detected.

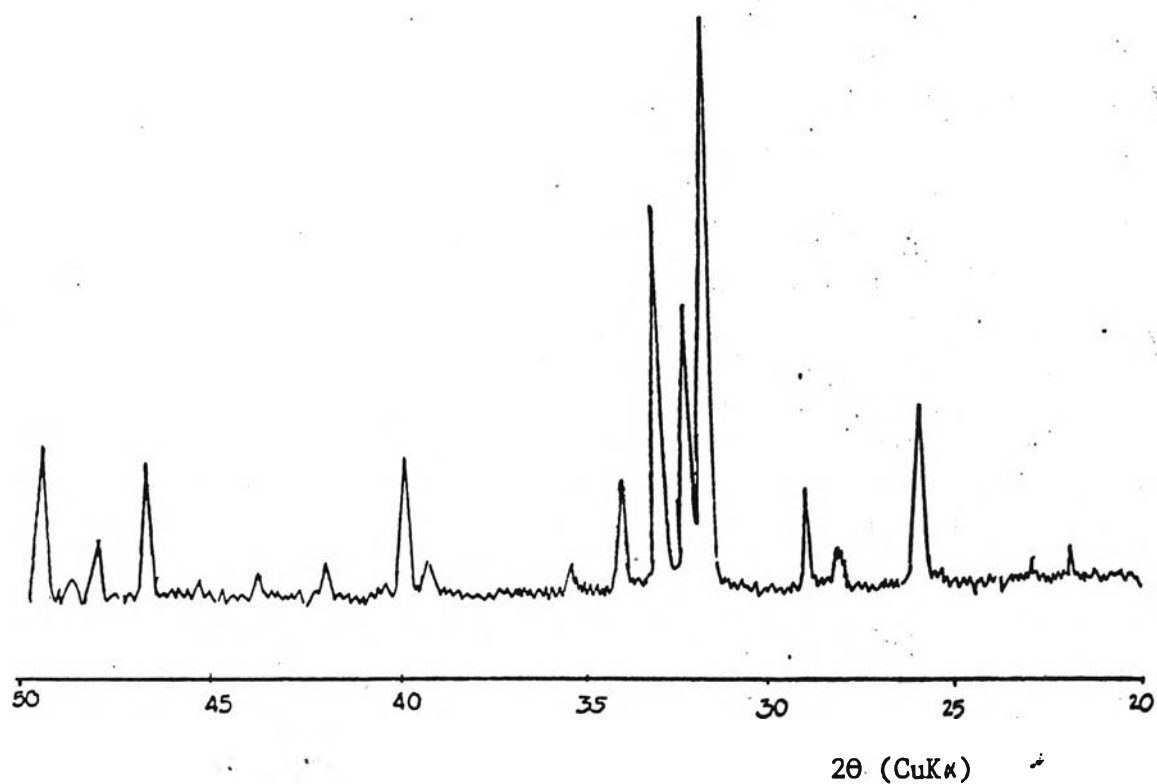


Fig. 13 XRD pattern of bone ash powder

(calcined at 700°C.3h)

#### 4.1.3 Infrared Spectra

The IR spectra from  $4000\text{--}370\text{ cm}^{-1}$  of the same sample using Nujol technique was shown in Fig. 14. The OH absorptions bands at  $3400\text{--}2600$  .  $630\text{ cm}^{-1}$  and  $\text{PO}_4^{3-}$  at  $1110\text{--}970\text{ cm}^{-1}$  in calcium hydroxyapatite were observed.

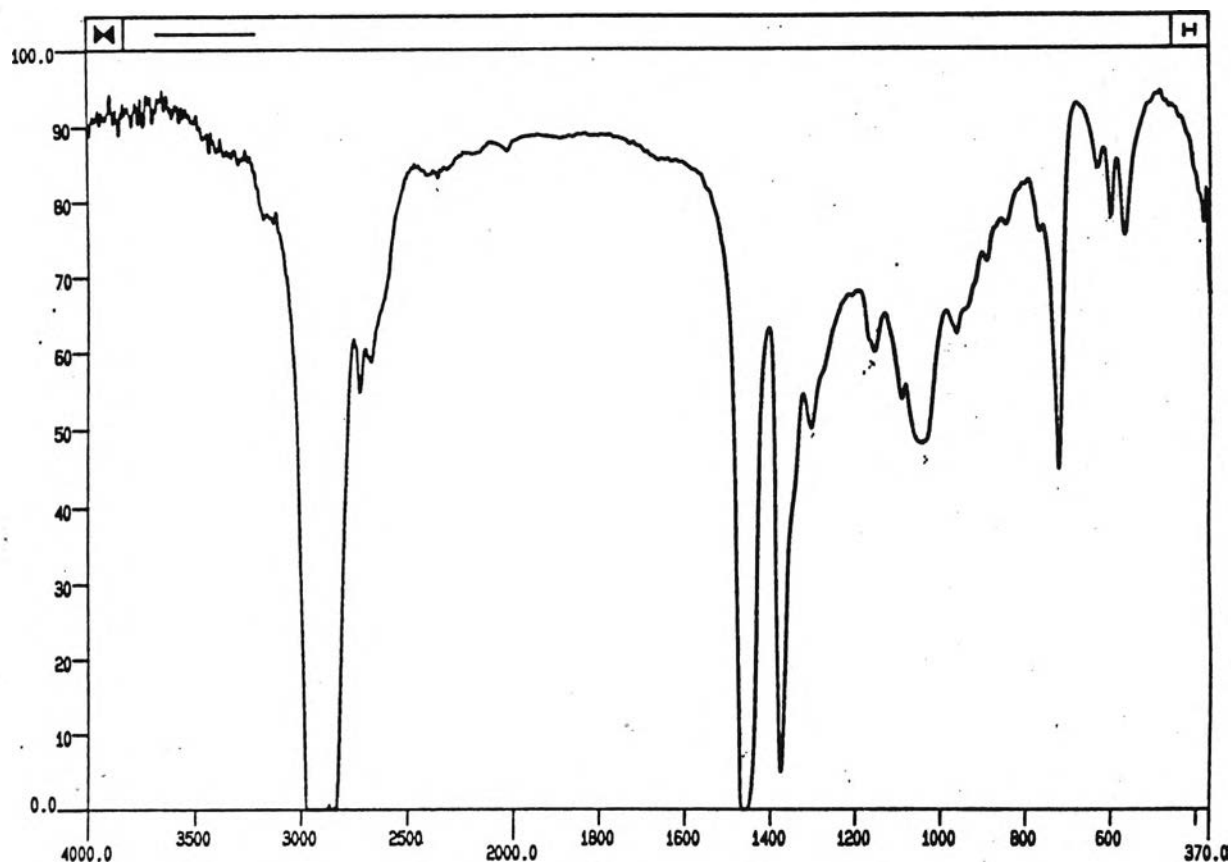


Fig. 14 Characteristic IR spectra of bone powder  
(calcined at  $700^\circ\text{C}$ . 3 h.)

## 4.2 Chemical Precipitation of DCPD

### 4.2.1 Phase Present in Precipitates from Various Conditions.

Characterization of the precipitates obtained from the reprecipitation of bone ash solution under various conditions. Phase present in the precipitates were detected by X-ray diffraction and the XRD patterns were shown in Fig. 15,16,17 and 18.

The set of d-spacing of  $11.7(2\theta=7.5^\circ)$ ,  $3.88(2\theta=22.9^\circ)$  and  $3.69(2\theta=24.1^\circ)$  agreed well with the powder diffraction card of monocalcium phosphate monohydrate (MCPM= $\text{Ca}(\text{H}_2\text{PO}_4)_2 \cdot \text{H}_2\text{O}$ ). No second phase was observed.

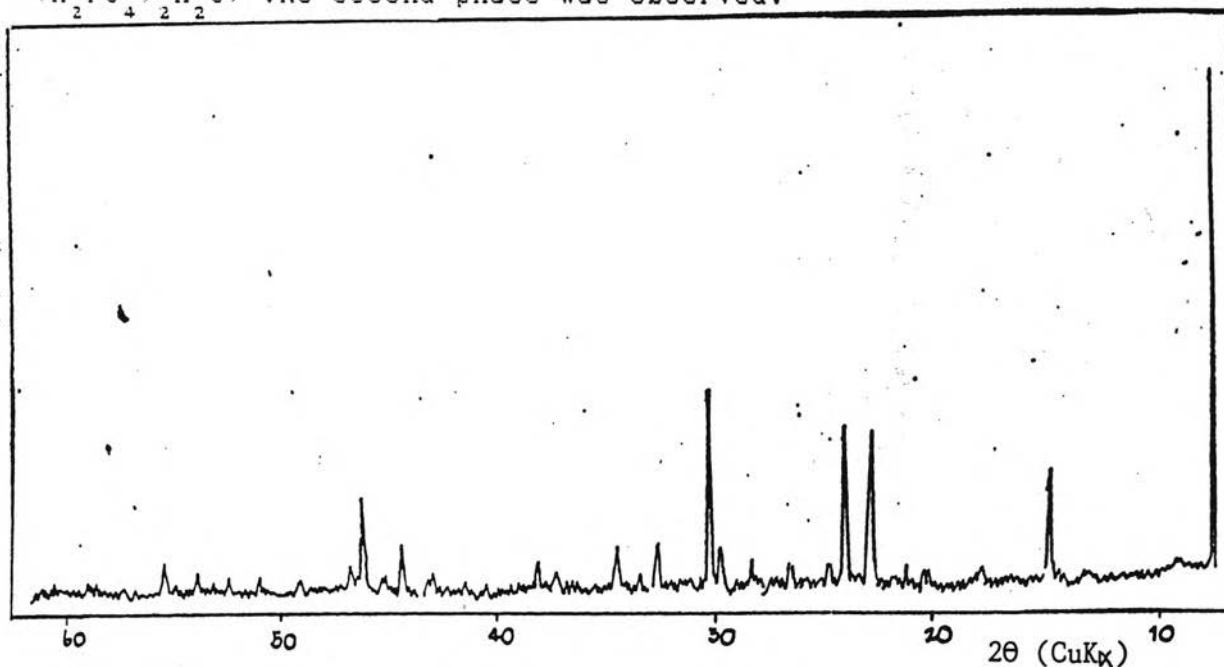


Fig.15 X-ray diffraction of precipitates (MCPM) obtained from a hot-saturated bone ash solution without Ca/P mole ratio adjustment .

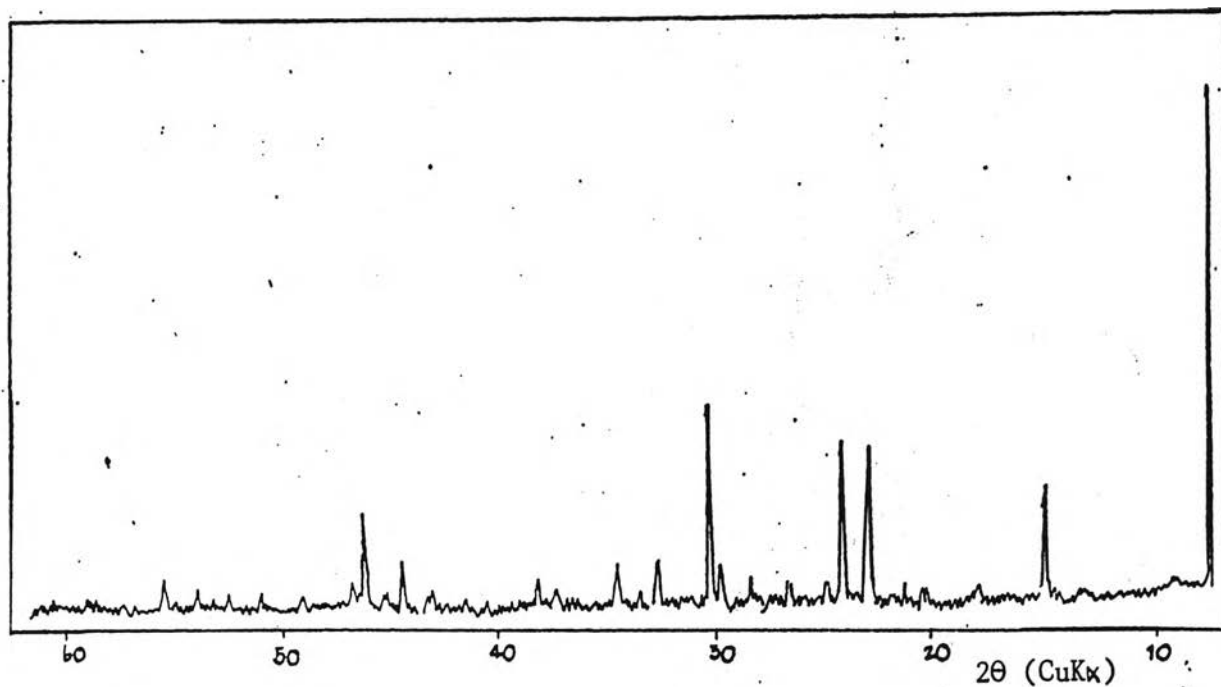


Fig.16 X-ray diffraction of precipitates (MCPM) obtained from a saturated bone ash solution at room temperature without Ca/P mole ratio adjustment.

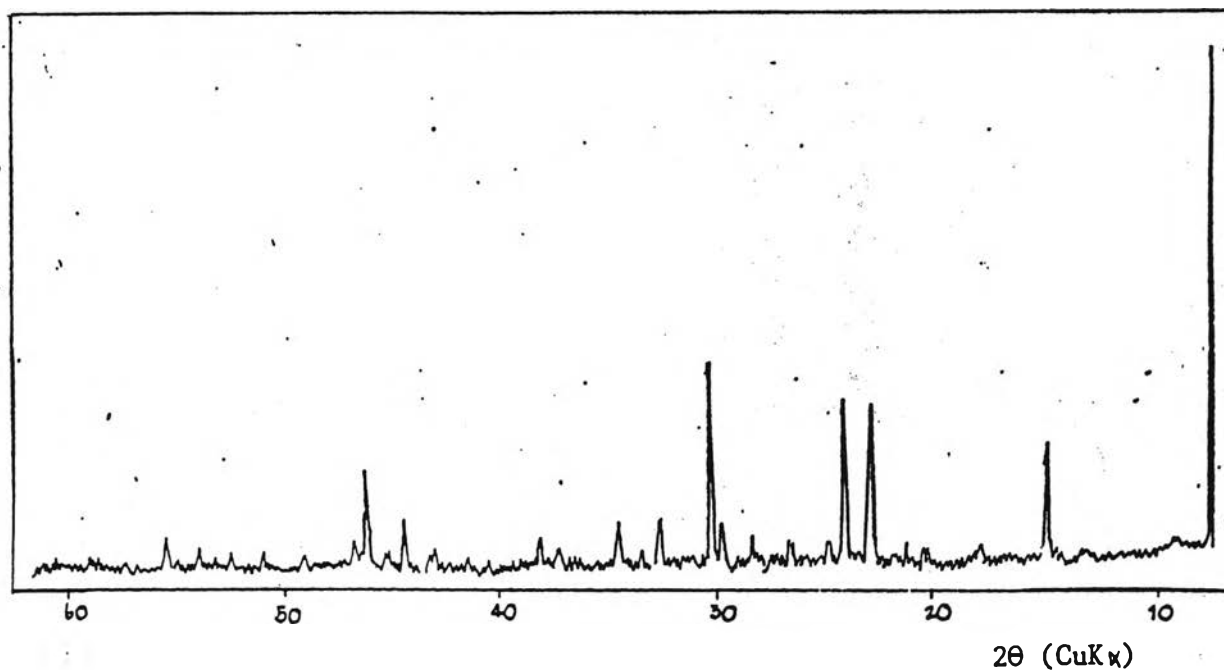


Fig.17 X-ray diffraction of precipitates (MCPM) obtained from a saturated bone ash solution at room temperature, adjusting Ca/P mole ratio by adding  $H_3PO_4$ .

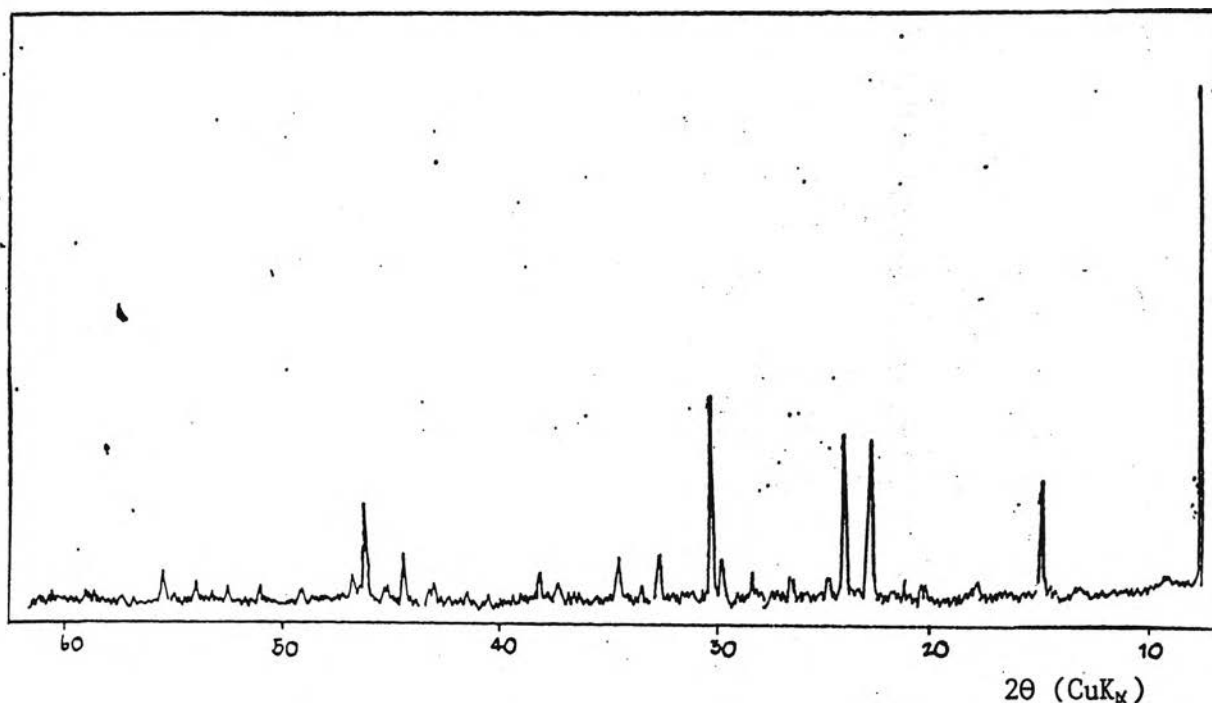


Fig.18 X-ray diffraction of precipitates (MCPM) obtained from a saturated bone ash solution at room temperature, adjusting Ca/P mole ratio by adding  $H_3PO_4$  and  $CaCl_2$ .

Fig. 19 showed the x-ray pattern of standard dicalcium phosphate dihydrate and Fig. 20, 21 and 22 showed the XRD patterns of precipitates obtained from the bone ash solution of which the pH was adjusted to 3.5, 4.0, 4.5, 5.0, 5.5 and 6.0 with  $1M.NH_4OH$ . The values of d-spacing were 7.57 ( $2\theta=11.6^\circ$ ), 3.05 ( $2\theta=29.2^\circ$ ) and 4.24 ( $2\theta=20.9^\circ$ ). They all agreed with those in the powder diffraction card of dicalcium phosphate dihydrate (DCPD:  $CaHPO_4 \cdot 2H_2O$ ) and no second phase was detected.

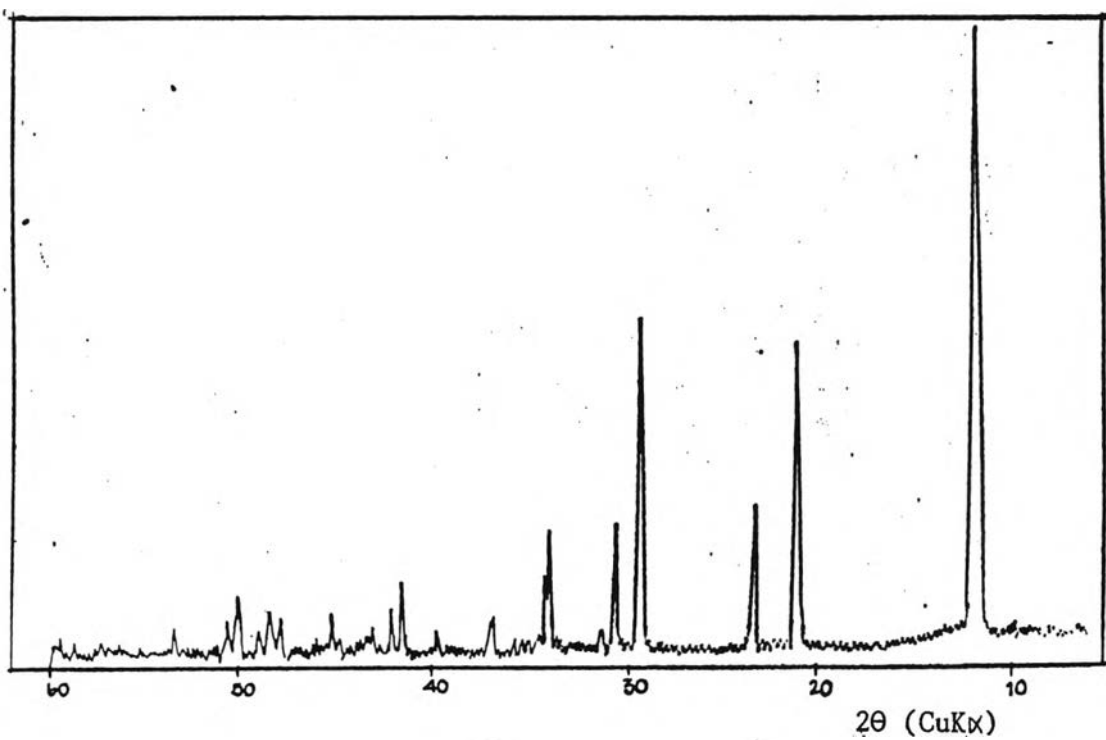
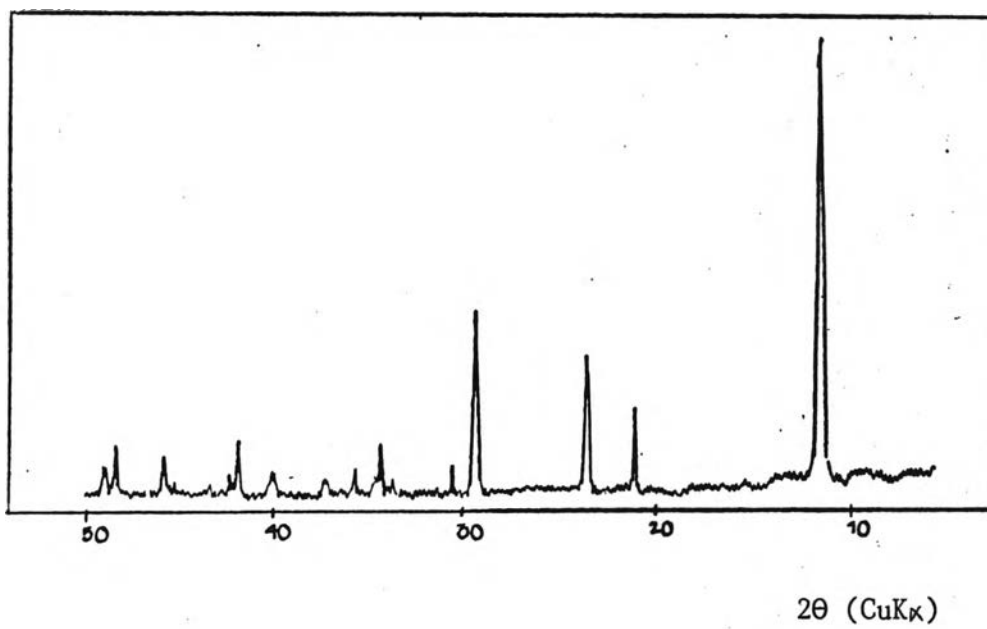
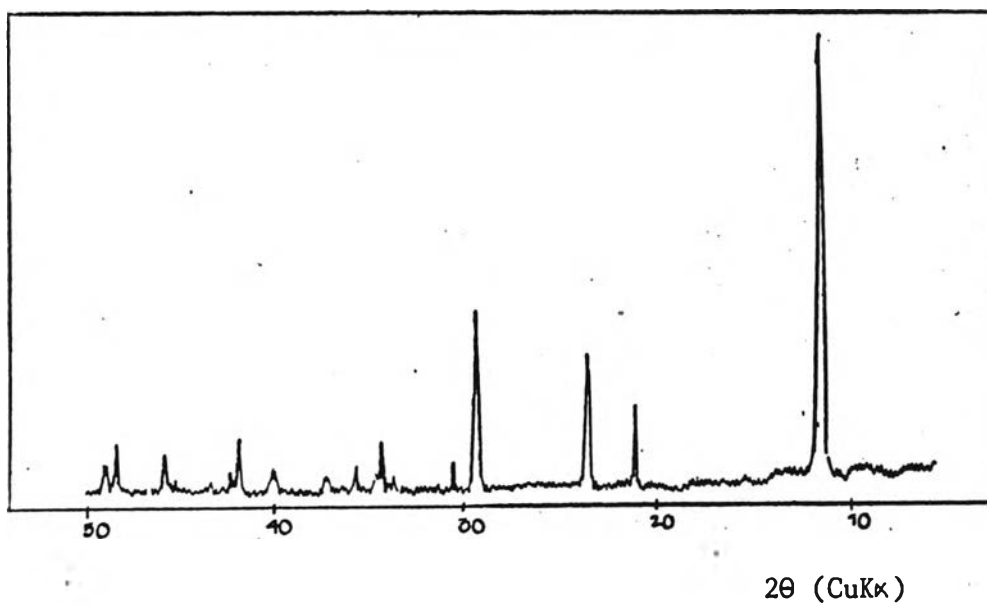


Fig. 19 X-ray diffraction of reference dicalcium phosphate dihydrate from Fluka :analyzed agent (>98%)

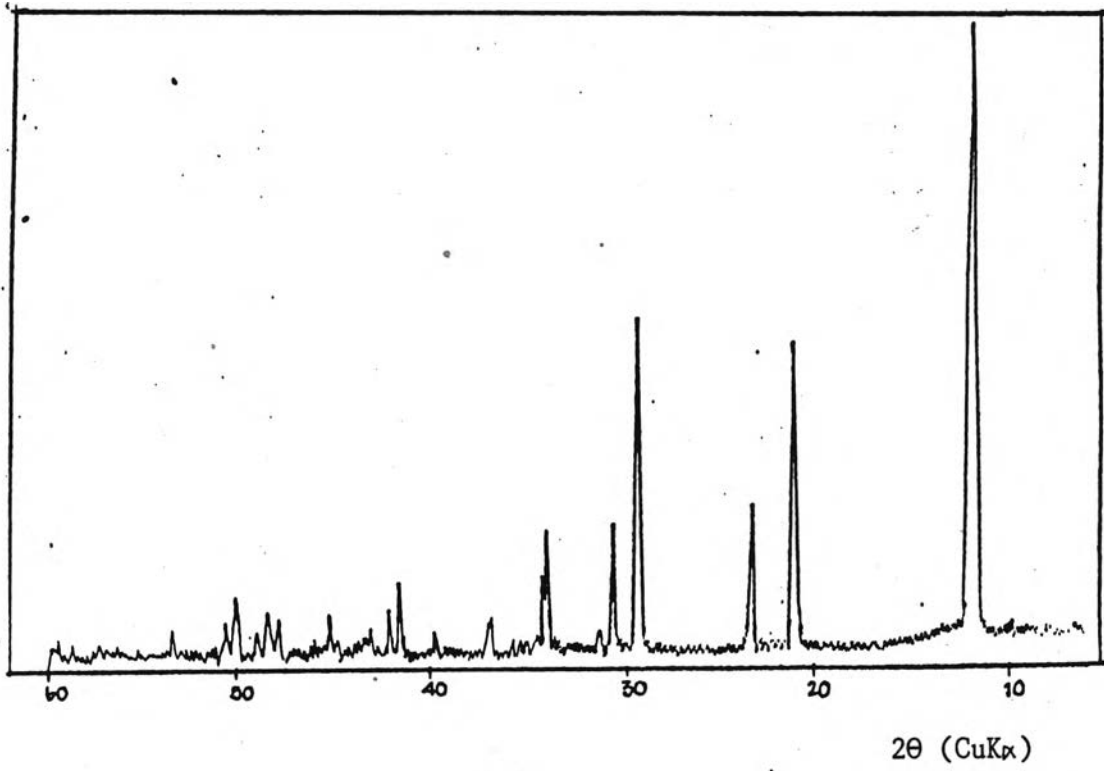




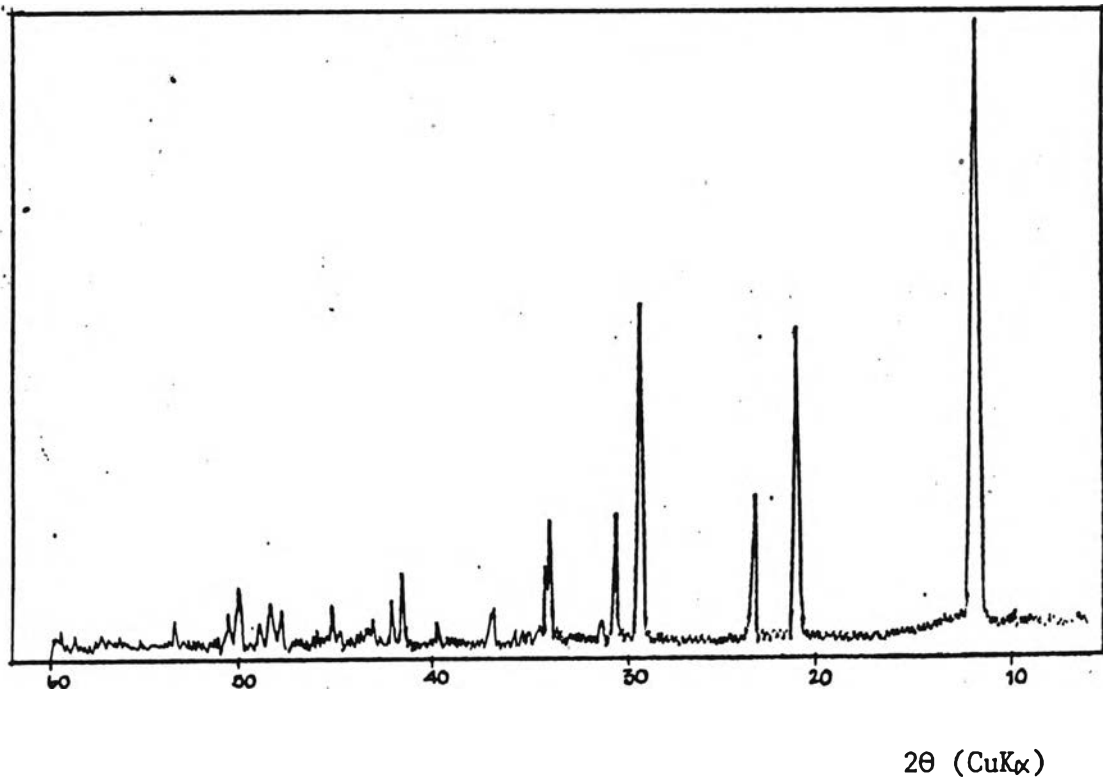
(a)



(b)



(c)



(d)

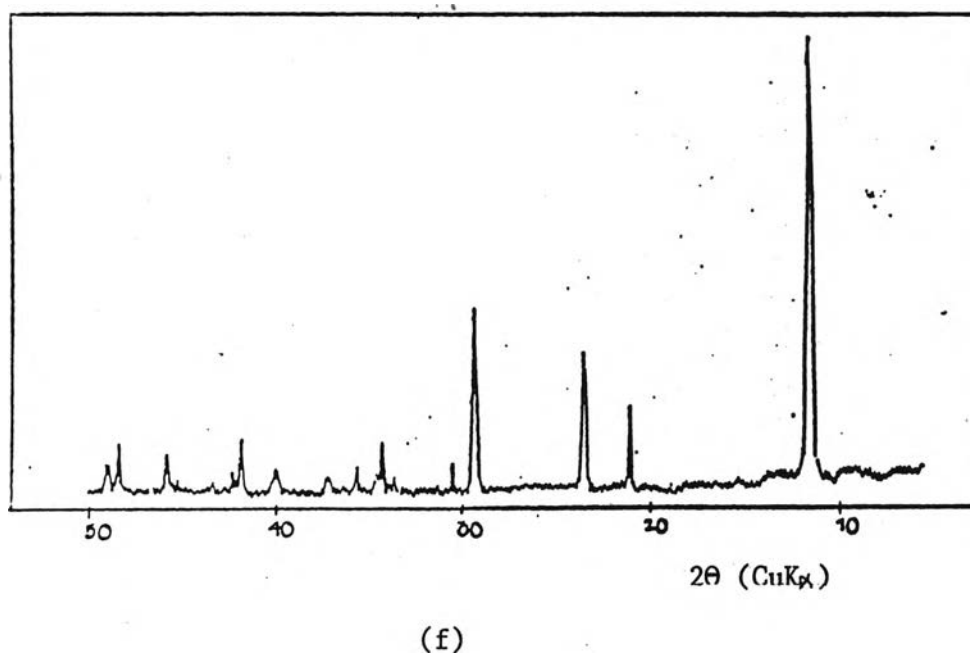
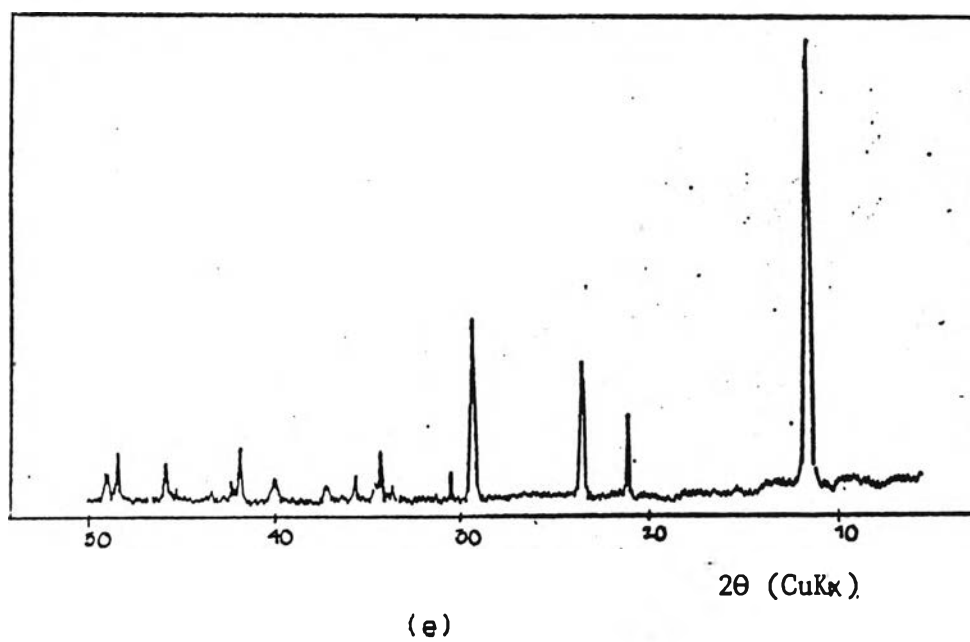
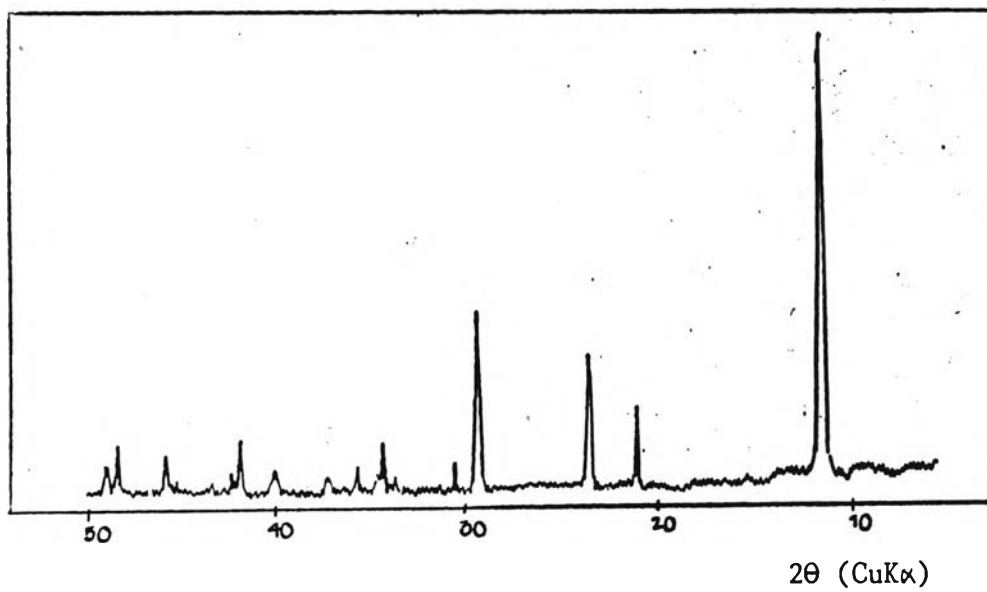
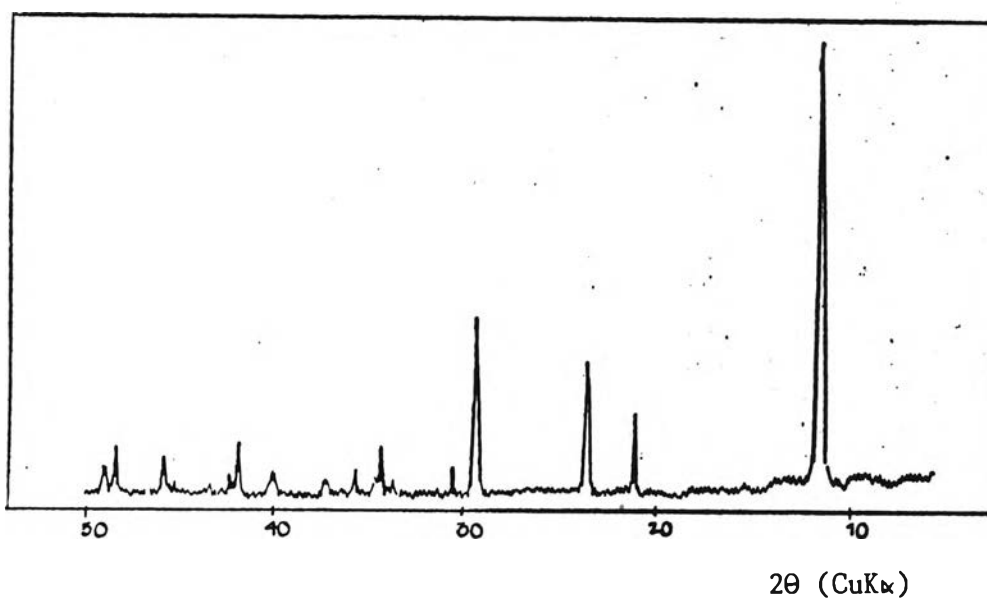


Fig.20 X-ray diffraction of precipitates (DCPD) obtained at pH 3.5, 4.0, 4.5, 5.0, 5.5 and 6.0 respectively, without Ca/P mole ratio adjustment.

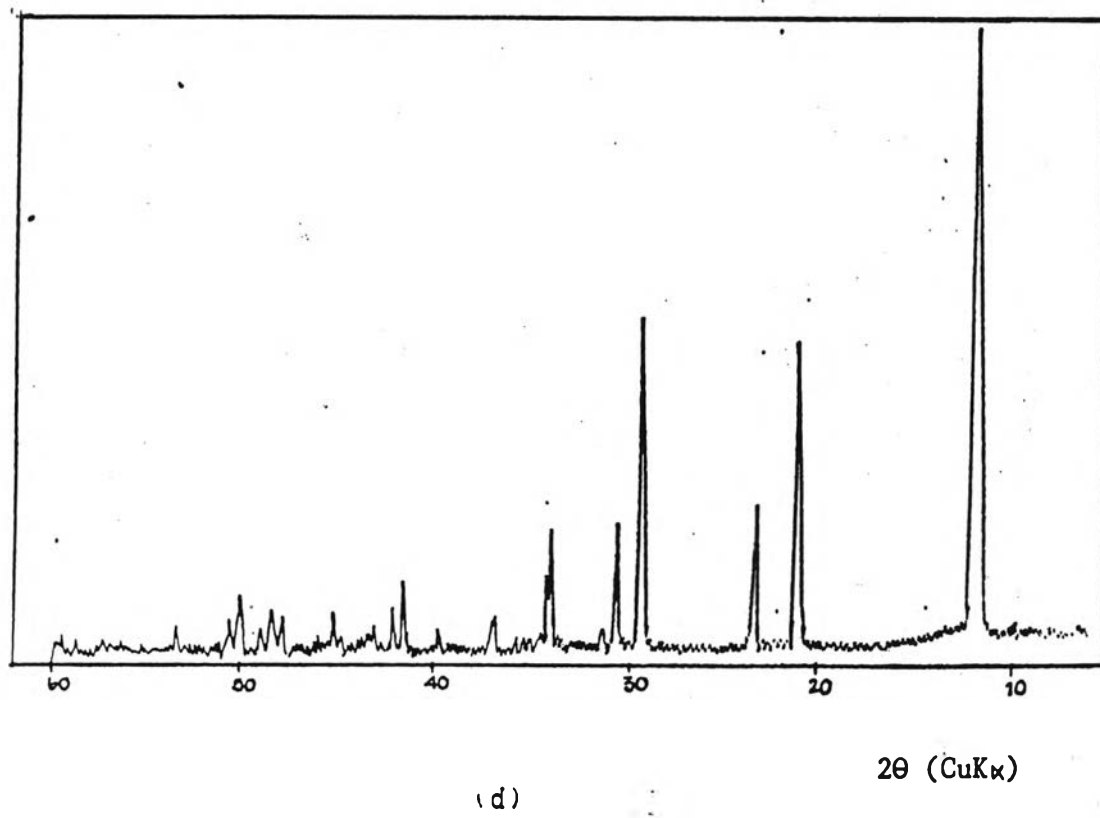
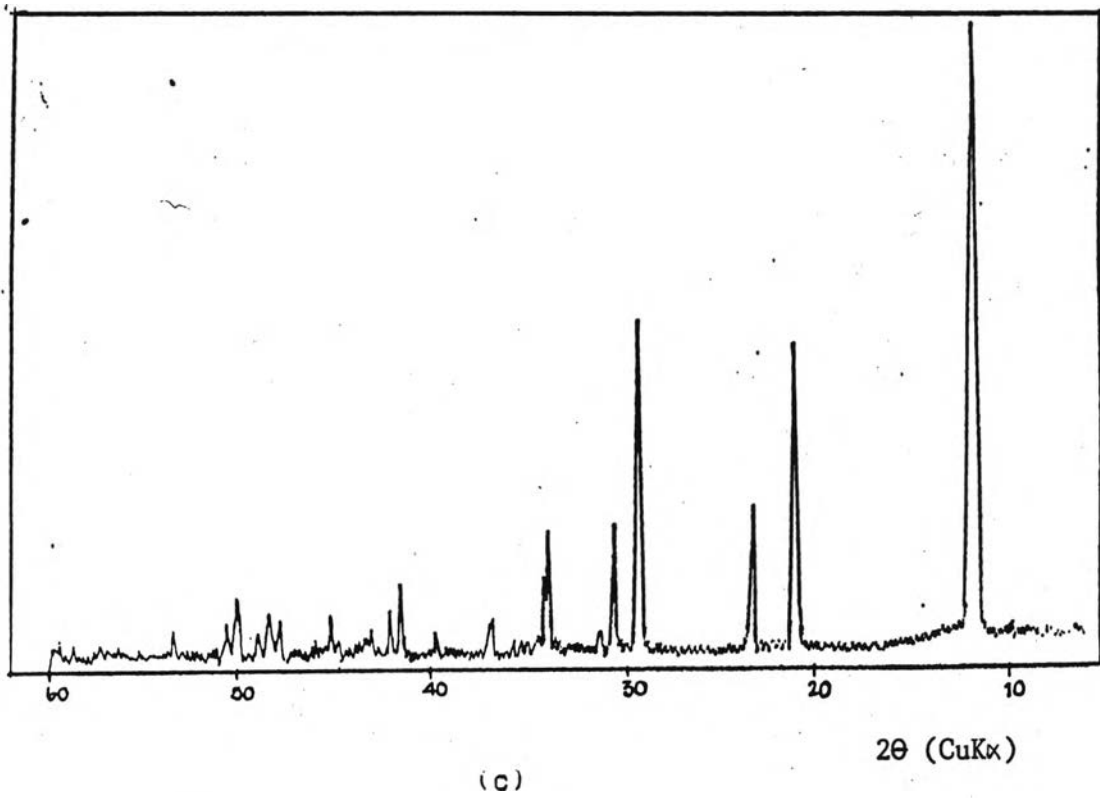
(a) pH=3.5, (b) pH=4.0, (c) pH=4.5,  
(d) pH=5.0, (e) pH=5.5, (f) pH=6.0



(a)



(b)



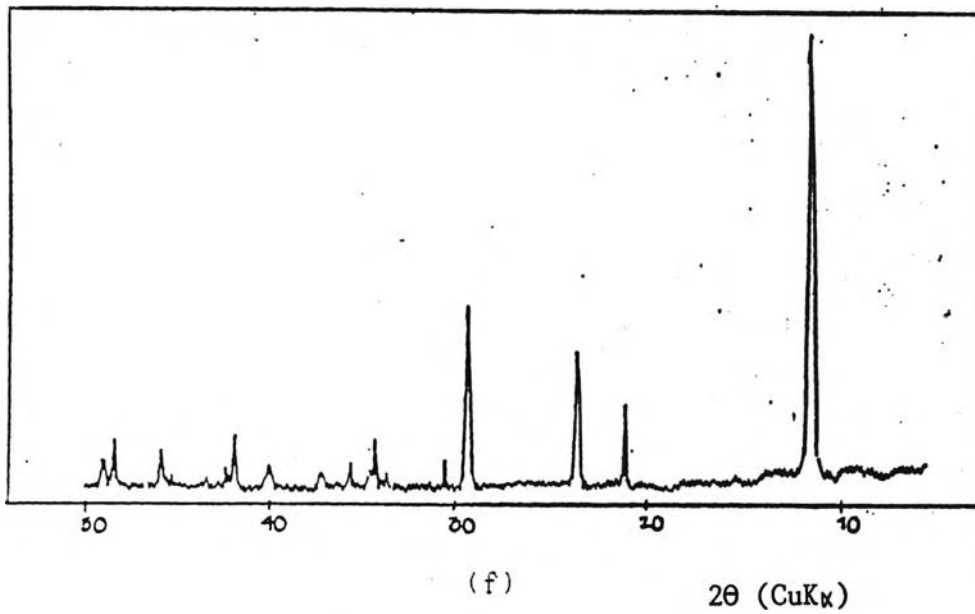
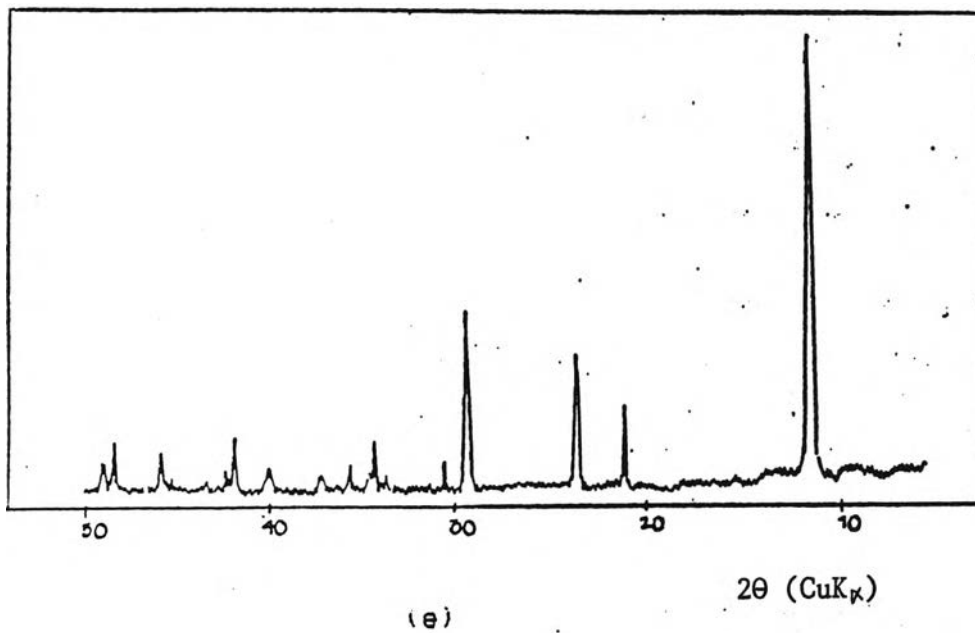
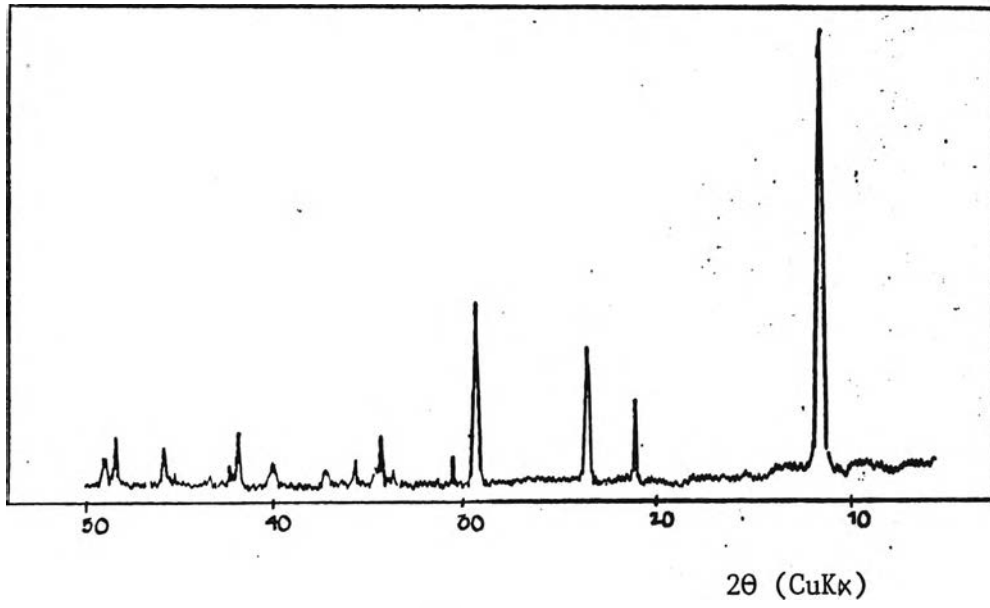


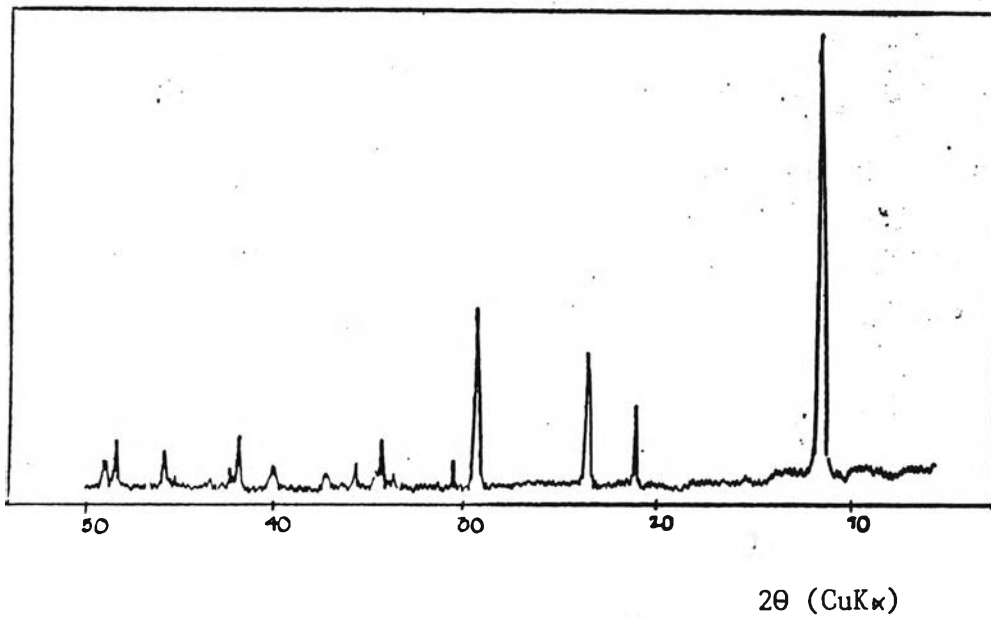
Fig.21 X-ray diffraction of precipitates (DCPD) obtained at pH 3.5, 4.0, 4.5, 5.0, 5.5, and 6.0 respectively, adjusting Ca/P mole ratio by adding  $H_3PO_4$ .

(a) pH=3.5, (b) pH=4.0, (c) pH=4.5

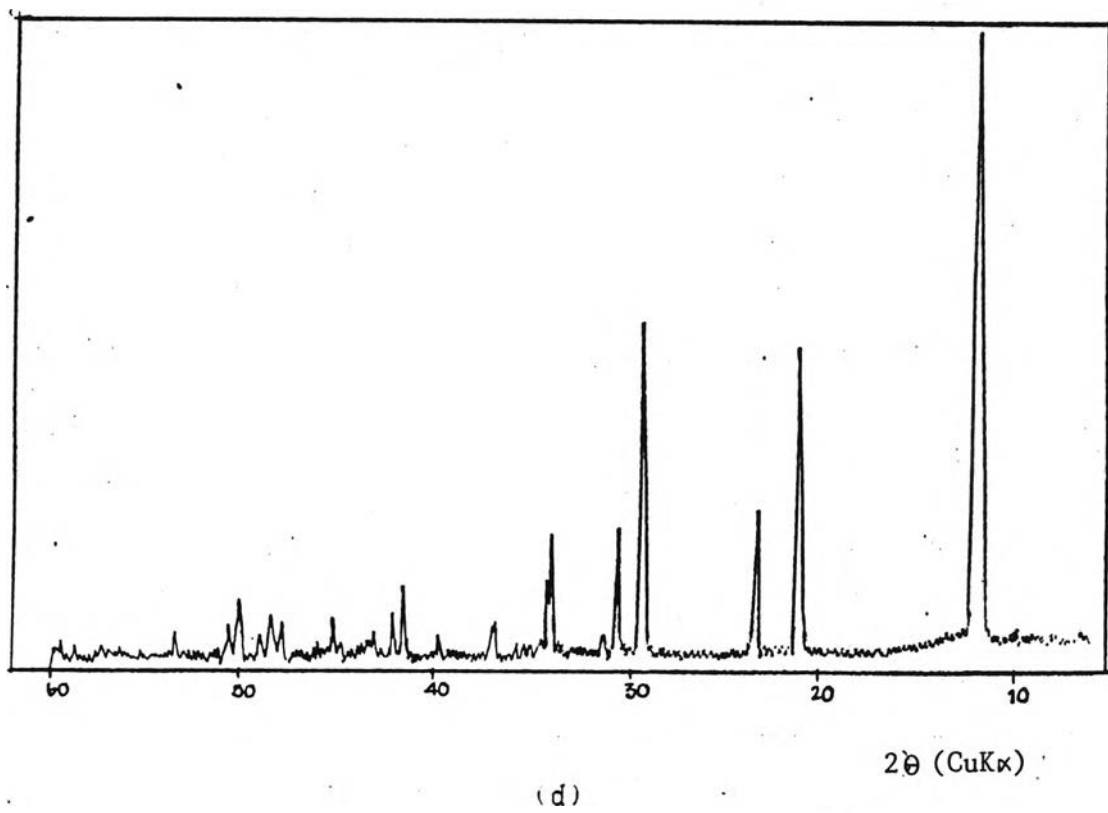
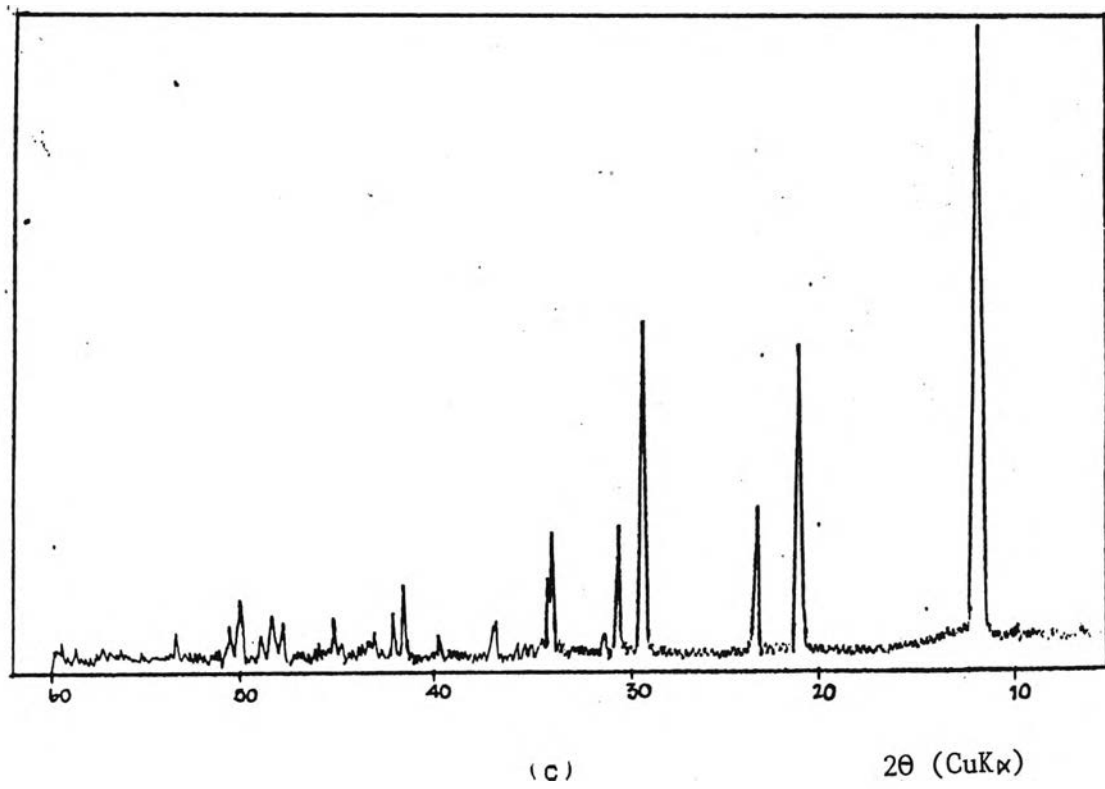
(d) pH=5.0, (e) pH=5.5, (f) pH=6.0



(a)



(b)





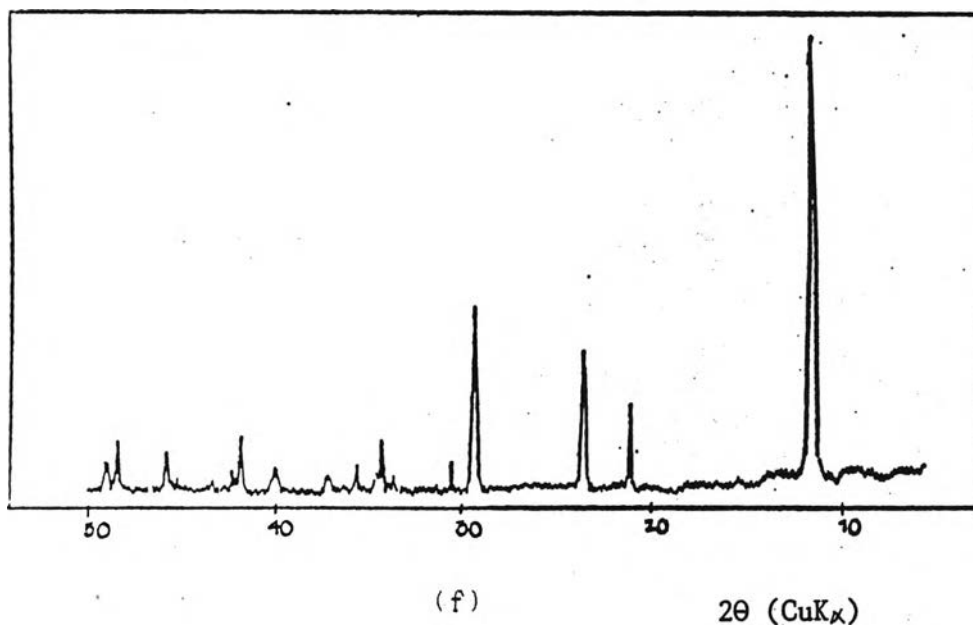
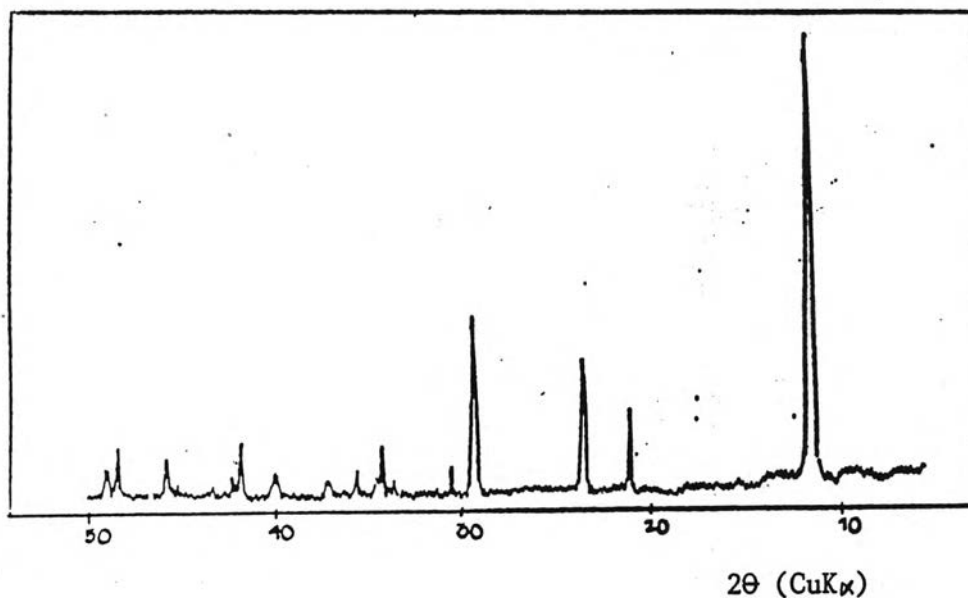


Fig. 22 X-ray diffraction of precipitates (DCPD) obtained at pH 3.5, 4.0, 4.5, 5.0, 5.5, and 6.0 respectively, adjusting Ca/P mole ratio by adding  $H_3PO_4$  and  $CaCl_2$ .  
(a) pH=3.5, (b) pH=4.0, (c) pH=4.5  
(d) pH=5.0, (e) pH=5.5, (f) pH=6.0

Table 11 Results of chemical precipitations of bone ash solution under various condition.

Condition		Phase present	
		by X-ray	
Ca/P mole ratio	Precipitation	diffraction	
Not-fixed	High temp.-Not adjusted pH	MCPM	
Ca/P mole ratio	Room temp.-Not adjusted pH	MCPM	
	-Adjusted to pH 3.5	DCPD	
	4.0	DCPD	
	4.5	DCPD	
	5.0	DCPD	
	5.5	DCPD	
	6.0	DCPD	
Fixed Ca/P mole ratio	Room temp.-Not adjusted pH	MCPM	
	-Adjusted to pH 3.5	DCPD	
	-by adding	4.0	DCPD
	$H_3PO_4$	4.5	DCPD
		5.0	DCPD
		5.5	DCPD
		6.0	DCPD

-by adding	Room temp.-Not adjusted pH	MCPM
$H_3PO_4 + CaCl_2$	-Adjusted to pH 3.5	DCPD
	4.0	DCPD
	4.5	DCPD
	5.0	DCPD
	5.5	DCPD
	6.0	DCPD

---

It was shown in Table 11 that the precipitates obtained from the precipitation without adjusting pH was only MCPM and DCPD was the only product in all the cases with adjusting pH in the range of 3.5 to 6.0. There was no significantly different effect on the obtained products from the solution that was control of Ca/P mole ratio by addition  $H_3PO_4$  acid or  $H_3PO_4 + CaCl_2$  and from the solution that was not controlled Ca/P mole ratio.

This could be explained from the solubility phase diagram (Fig.23: a.b ,the solubility phase diagram of ternary system  $Ca(OH)_2 - H_3PO_4 - H_2O$ .(Laurence C.Chow and Walter E.Brown, 1975). The solution above the isotherms were saturated and those below were undersaturated with respect to a solid.

The isotherm of OHAp and DCPD shown in Fig.23,b appeared to overlap over a range of compositions, but in

Fig.23.a the corresponding positions of the isotherms were well separated. Thus a solution saturated with respect to OHAp would have nearly the calcium and phosphate concentration as those of a solution saturated with respect to DCPD, but the pH of two solutions would be considerably different. Therefore in the precipitation of DCPD from a bone ash solution (Ca-deficient hydroxyapatite, Fig.13), pH was an important parameter. This had been proved by the result obtained in Table 11. At point S (which was sometimes called the singular point), where the isotherms of OHAp and DCPD intersect, the solution was saturated with respect to both solids. Similarly, at point T the solution is simultaneously saturated with respect to both DCPD and  $\text{Ca}(\text{H}_2\text{PO}_4)_2 \cdot \text{H}_2\text{O}$ .

OHAp was known to be much less soluble (or more stable) than DCPD under most conditions in vivo, which would be in the lower right and left portions of Fig.23,a,b respectively. It could be seen that the reverse was true, however, for solutions more acidic than the singular point solution. Under these conditions on the DCPD isotherm in Fig.23.a was undersaturated with respect to OHAp. Point C lied on the DCPD isotherm and not on the OHAp isotherm even though this fact was not apparent in Fig. 23,b where the two isotherms appeared nearly superimposed. OHAp contacting

solution C would therefore tend to dissolve ,and as a result, the solution composition would move from C to a point slightly above the DCPD isotherm. Since the resulting solution would be supersaturated with respect to DCPD, precipitation of DCPD would occur so that the solution composition would be brought back to the DCPD isotherm at, for example, E in Fig.23,b. Point E lied below C because the dissolving solid ;DCPD, this yielded a resulting solution that was less acidic than the initial solution. OHAp would continue to dissolve and DCPD would precipitate as long as OHAp was available , or until the solution composition reached the singular point S . In the latter instance an equilibrium situation obtained because the solution had become saturated with respect to both OHAp and DCPD. It was seen that the DCPD solution, in which the dissolution of OHAp and precipitation of OHAp and DCPD took place , always became more dilute (and also less acidic) as a result of the reaction. In other words, the amount of DCPD precipitated from the solution was greater than that of OHAp dissolved.

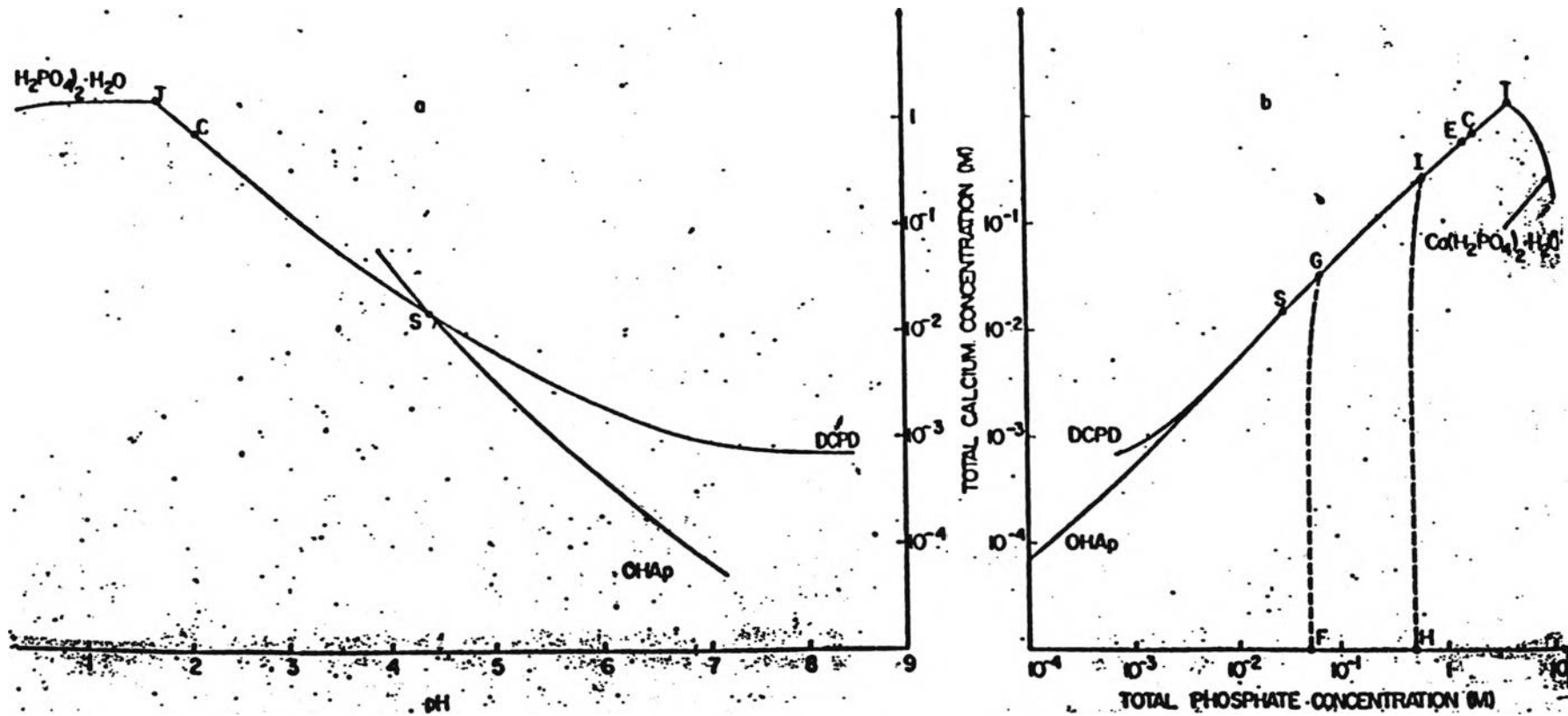


Fig. 23 Solubility phase diagram of ternary system  $\text{Ca}(\text{OH})_2\text{-H}_3\text{PO}_4\text{-H}_2\text{O}$ .

Moreover different calcium phosphate phase might be stabilized or destabilized by presence of various cations and anions. For example, in the same conditions magnesium ions played an important role in inhibiting the precipitation of OHAp (P. Christel and A. Meunier, 1986). This result might be a one of factors that dicalcium phosphate dihydrate could precipitate at pH greater than point S, e.g., pH 6 with no second phase of OHAp.

#### 4.2.2 pH Effect.

This study was attempted to find out the suitable pH for the precipitation of DCPD from various bone ash solutions. From the analysis of X-ray diffraction pattern, dicalcium phosphate dihydrate was obtained from bone ash solution that was adjusted to 3.5 to 6.0. The relation between pH of bone ash solution and weight of dicalcium phosphate dihydrate was shown in Fig.24. The products from each conditions was detected by XRD and it was found that DCPD was obtained from the precipitation of which pH was 3.5-6.0 e.g., DCPD obtained from solution was not fixed Ca/P mole ratio solution, fixed Ca/P mole ratio by adding  $H_3PO_4$  and fixed Ca/P mole ratio by adding  $H_3PO_4$  and  $CaCl_2$  as seen in Fig. 24.

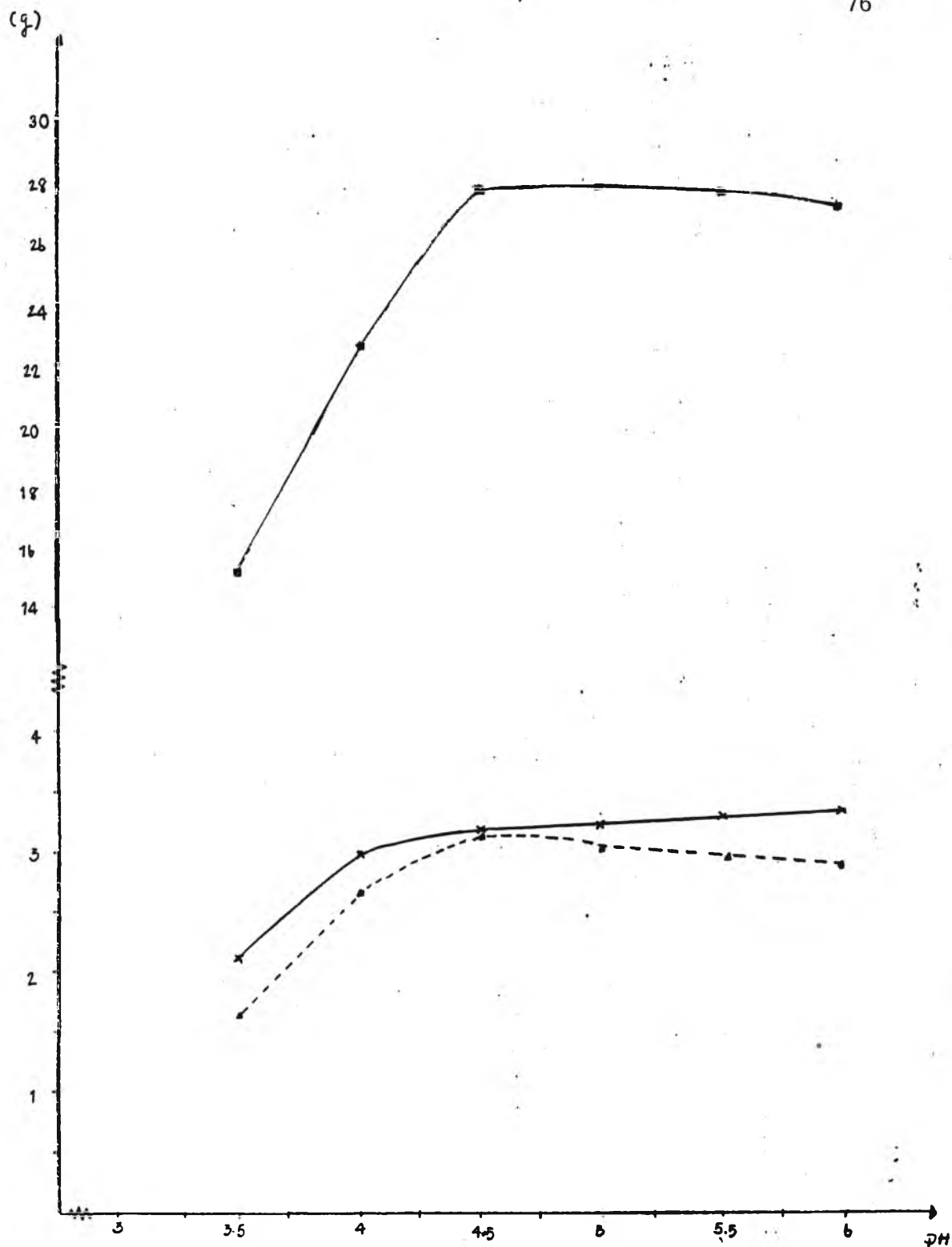


Fig. 24 Relation between weight(g) of DCPD and pH

× Not adjusted Ca/P mole ratio

▲ Adjusted Ca/P mole ratio by adding  $H_3PO_4$

■ Adjusted Ca/P mole ratio by adding  $H_3PO_4 + CaCl_2$



Results in Fig.24 showed that the maximum amount of DCPD in the maintained condition was at around 4.5-5.5. This meant that in the pH range 4.5-5.5, DCPD was the most stable phase. The maximum amount of DCPD from bone as solution which was not fixed Ca/P mole ratio and fixed mole ratio by adding  $H_3PO_4$  was close to each other but the yield of DCPD obtained from solution that was fixed Ca/P mole ratio by adding  $H_3PO_4$  and  $CaCl_2$  was very large because large volume of both  $H_3PO_4$  and  $CaCl_2$  was added in order to control the Ca/P mole ratio.

4.2.3 Ca /P Mole Ratio and Impurities of Dicalcium Phosphate Dihydrate at pH 4.5-5.5 from Bone Ash Solution Without Fixing Ca/P Mole Ratio.

In order to narrow the pH of precipitation, products from solution that was not fixed Ca/P mole ratio and solution that was fixed Ca/P mole ratio by adding  $H_3PO_4$  were analyzed from impurities and Ca/P mole ratio. The results were tabulated in Table 12, 13 ( The solution that was fixed Ca/P mole ratio by adding  $H_3PO_4$  and  $CaCl_2$  was not chosen because it was not convenient and economic).

Table 12 show Ca/P mole ratio and amount of impurities, of precipitates obtained at pH 4.5-5.5 from without Ca/P mole ratio adjustment of bone as solution characterized by Mineral Assay and Service

Characteristic	Precipitation , pH		
	4.5	5.0	5.5
Ca/P mole ratio	1.06/1	1.06/1	1.1/1
Impurities, Mg(%)	0.01	0.01	0.01
Fe(%)	0.07	0.17	0.07
Zn(ppm)	38	30	61
Cu(ppm)	3	2	4
Mn(ppm)	5	5	5
Heavy metals, Cd(ppm)	< 0.5	< 0.5	< 0.5
Pb(ppm)	< 5	< 5	< 5
Hg(PPM)	< 1	< 1	< 1
As(ppm)	< 0.5	< 0.5	< 0.5
Ni(ppm)	2	2	2

Table 13 show Ca/P mole ratio and amount of impurities, of precipitates obtained at pH 4.5-5.5 from adjusted bone ash solution by adding  $H_3PO_4$  characterized by Mineral Assay and Service.

Characteristic	Precipitation ,pH		
	4.5	5.0	5.5
Ca/P mole ratio	0.93/1	0.95/1	0.96/1
Impurities, Mg(%)	0.01	0.01	0.01
Fe(%)	0.01	0.01	0.01
Zn(%)	68	67	65
Cu(%)	5	5	5
Mn(%)	5	5	5
Heavy metals, Cd(ppm)	< 0.5	< 0.5	< 0.5
Pb(ppm)	< 5	< 5	< 5
Hg(ppm)	< 1	< 1	< 1
As(ppm)	< 0.5	1.5	< 0.5
Ni(ppm)	2	2	2

The values of Ca/P mole ratio obtained in Table 12 and 13 are all close to 1:1 which correspond to that of DCPD and also confirmed by XRD pattern Fig. 20, 21. The quantity of impurities in the obtained product in the pH range 4.5-5.5 with and without Ca/P mole ratio adjustment showed no significant difference. The amount of impurities present in DCPD products was well within the limit of ASTM: 1088-87.

From all the results obtained, the possibility to prepared DCPD at low cost from cattle bone was to precipitate DCPD at pH 4.5 from bone ash solution that was adjusted Ca/P mole ratio by adding  $H_3PO_4$  and  $HNO_3$ .

### 4.3 Tricalcium Phosphate

#### 4.3.1 DTA Study

In Fig. 25, the DTA curve of stoichiometric mixture between the prepared dicalcium phosphate dihydrate and calcium carbonate was shown.

It showed many reaction steps that occurred when stoichiometric mixture was heated up to 1350°C in air at a heating rate of 5°C/min. An endothermic peak was observed at temperature in the range of 105-185°C and a few exothermic peaks at temperature between 225-325°C caused by the liberation of water. At 420-450°C, an exothermic peak caused by decomposition of  $\text{CaHPO}_4$  to  $\text{Ca}_2\text{P}_2\text{O}_7$  was observed. Around temperature 800-860°C the liberation of carbon dioxide from calcium carbonate and dissociation of  $\text{Ca}_2\text{P}_2\text{O}_7$  to  $\beta$ -TCP were shown as endothermic peaks and  $\beta$ -TCP converted endothermically into  $\alpha$ -TCP at about 1155-1220°C.

To confirm the conversion, the DTA curve of  $\beta$ -TCP that was heated up to 1350°C in air at a heating rate of 5°C/min was shown in Fig.26. The only endothermic peak at 1155-1220°C,  $\beta$  to  $\alpha$ -TCP conversion was observed.

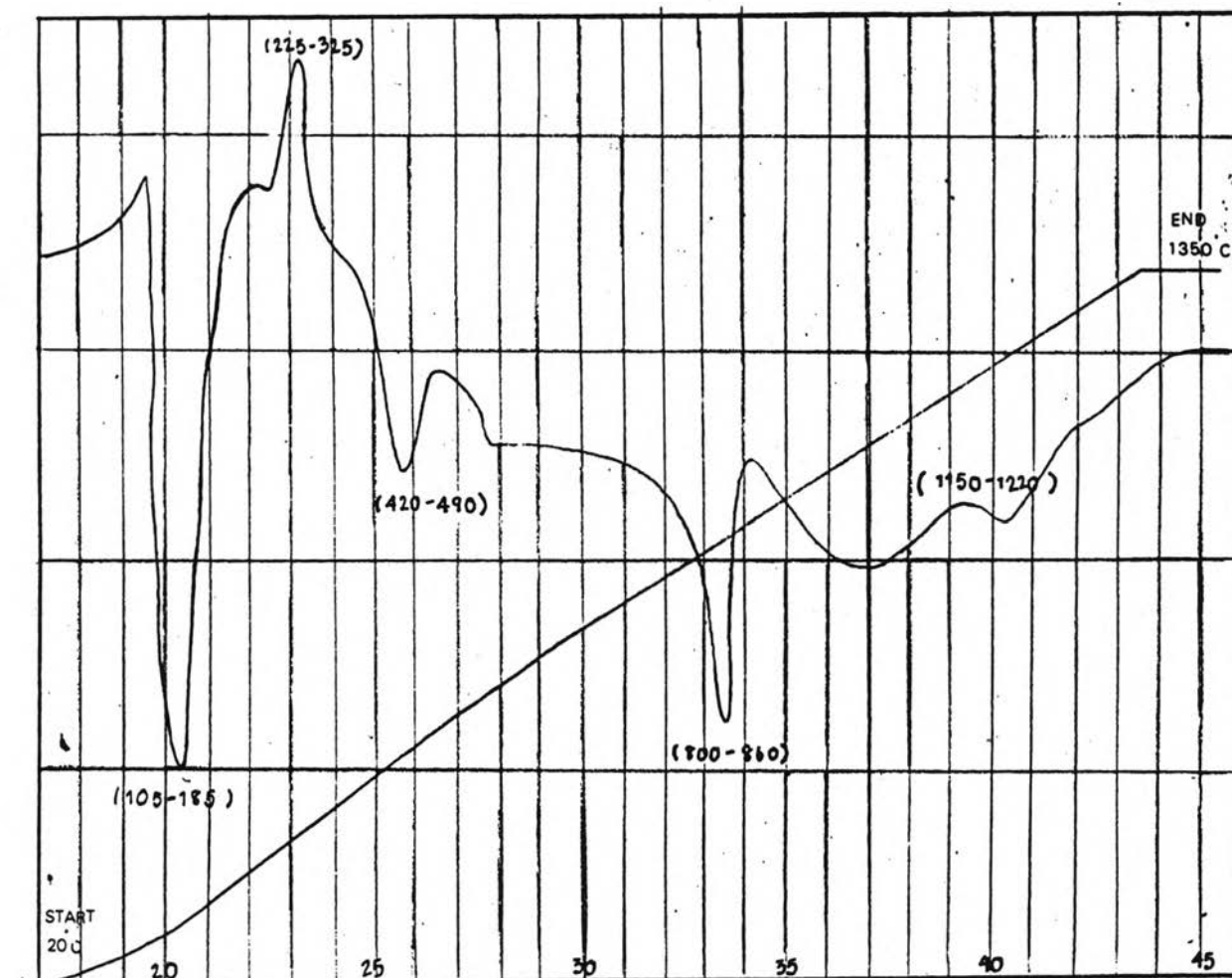


Fig.25 DTA curve of stoichiometric mixture between the prepared DCPD and calcium carbonate, heating rate 5 °C/ min.

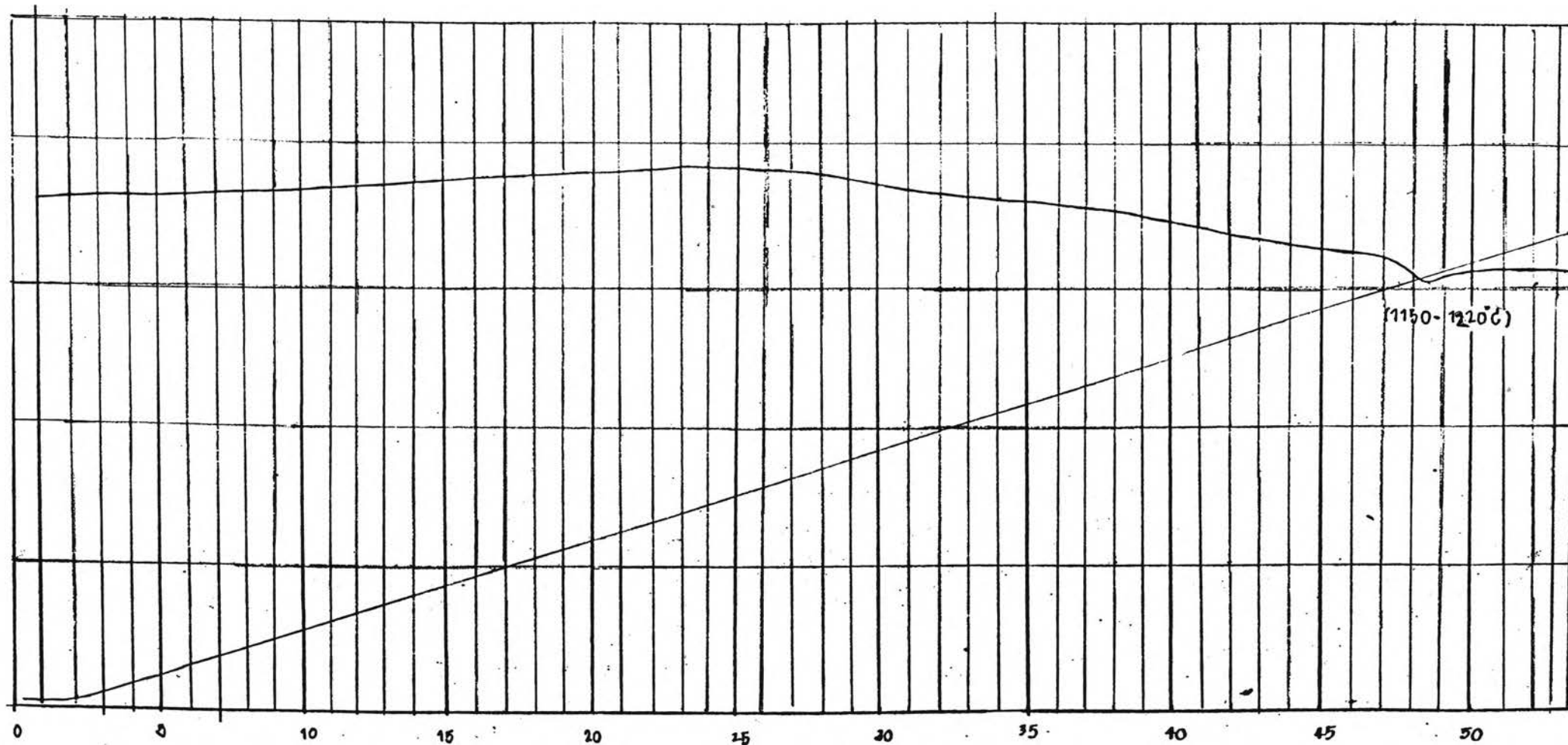
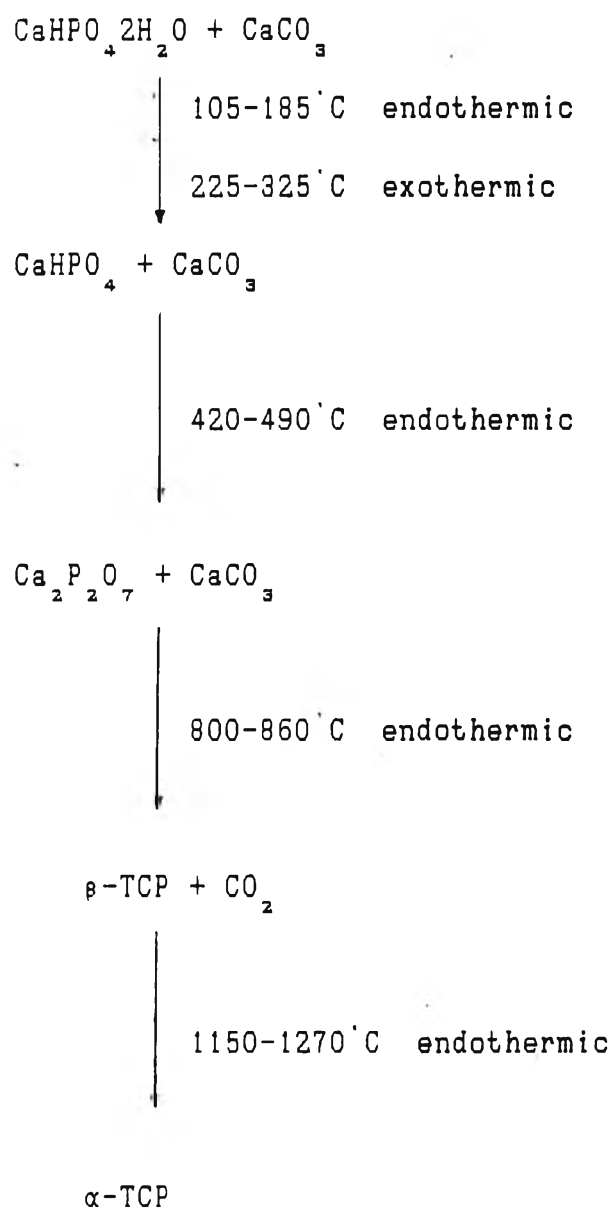


Fig. 26 DTA curve of prepared  $\rho$ -TCP, heating rate 5°C



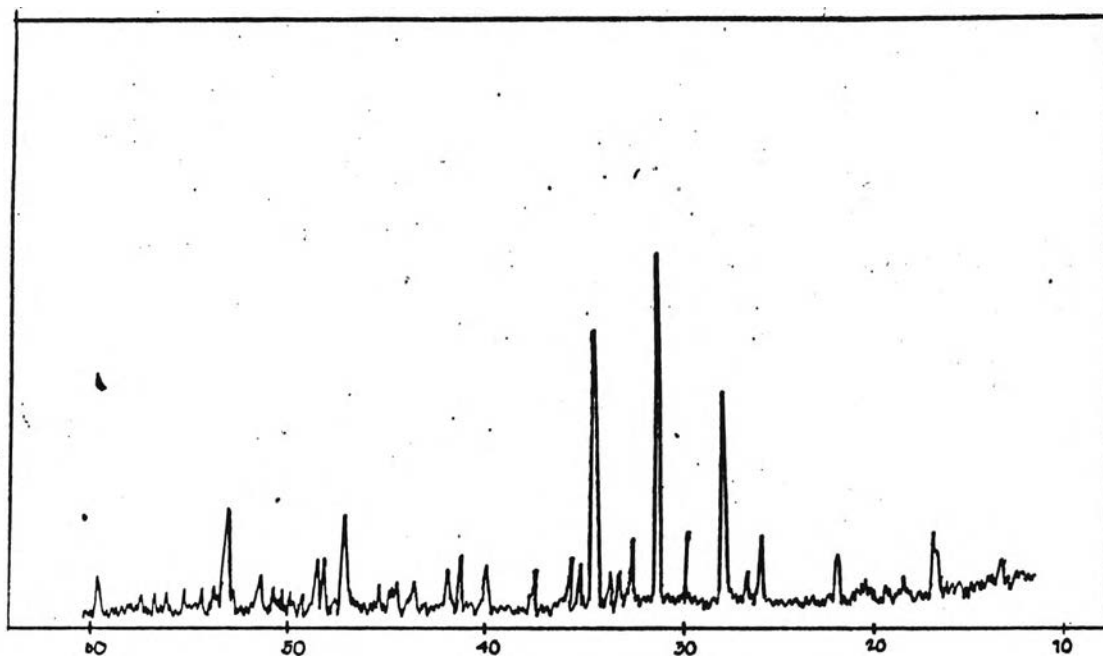
The reactions taking place during heating of the stoichiometric mixture of DCPD +  $\text{CaCO}_3$  powder could be summarized as follows:



#### 4.3.2 Phases present

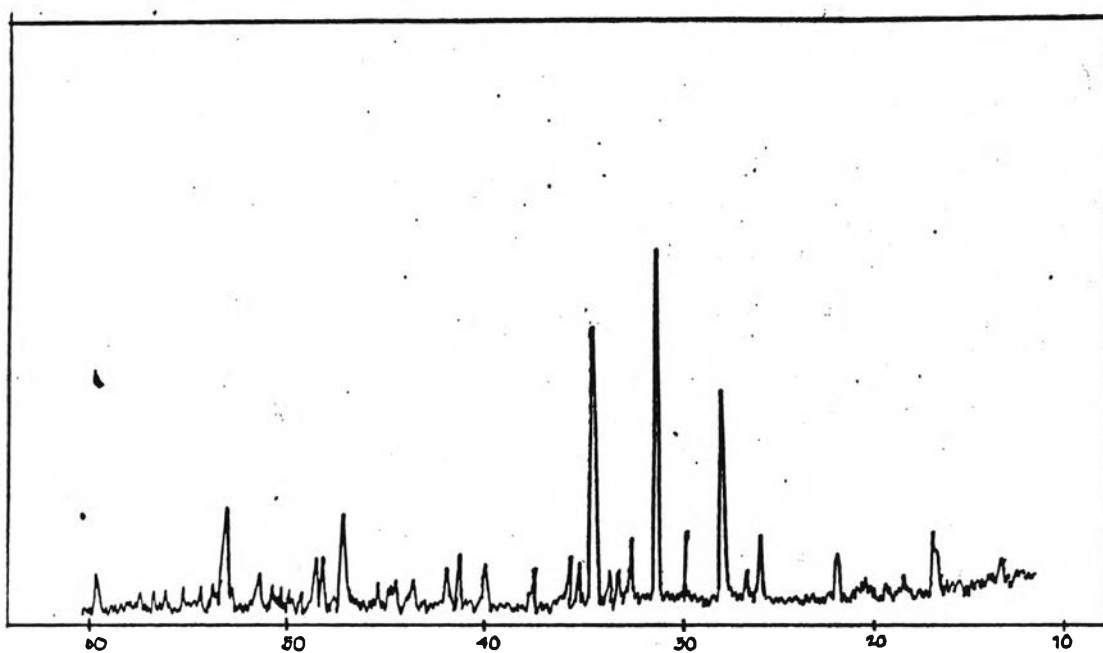
The XRD patterns of both prepared DCPD and reference DCPD stoichiometrically mixed with calcium carbonate heated at 1100°C with and without quenching in air was shown in Fig. 27: a, b and 28: a, b. They were all identified as  $\beta$ -tricalcium phosphate, ( $\beta$ -Ca<sub>3</sub>(PO<sub>4</sub>)<sub>2</sub>) with d-spacing of 2.88 (2 $\theta$ =31.0°), 2.607 (2 $\theta$ = 34.4°) and 3.21 (2 $\theta$ =27.8°) respectively.

Further firing to 1200°C, the product partly transformed to  $\alpha$ -tricalcium phosphate ( $\alpha$ -Ca<sub>3</sub>(PO<sub>4</sub>)<sub>2</sub>) with d-spacing of 2.905(2 $\theta$ =30.8°), 3.91(2 $\theta$ =22.7°) and 3.88(2 $\theta$ =22.9°) which were shown in Fig.29:a,b and 30:a,b. The quantity of  $\alpha$ -TCP increased with temperature up to 1300°C, as shown in Fig. 31: a, b and 32: a, b. Both air-quenched and slowly cooled products gave the same result.



(a)

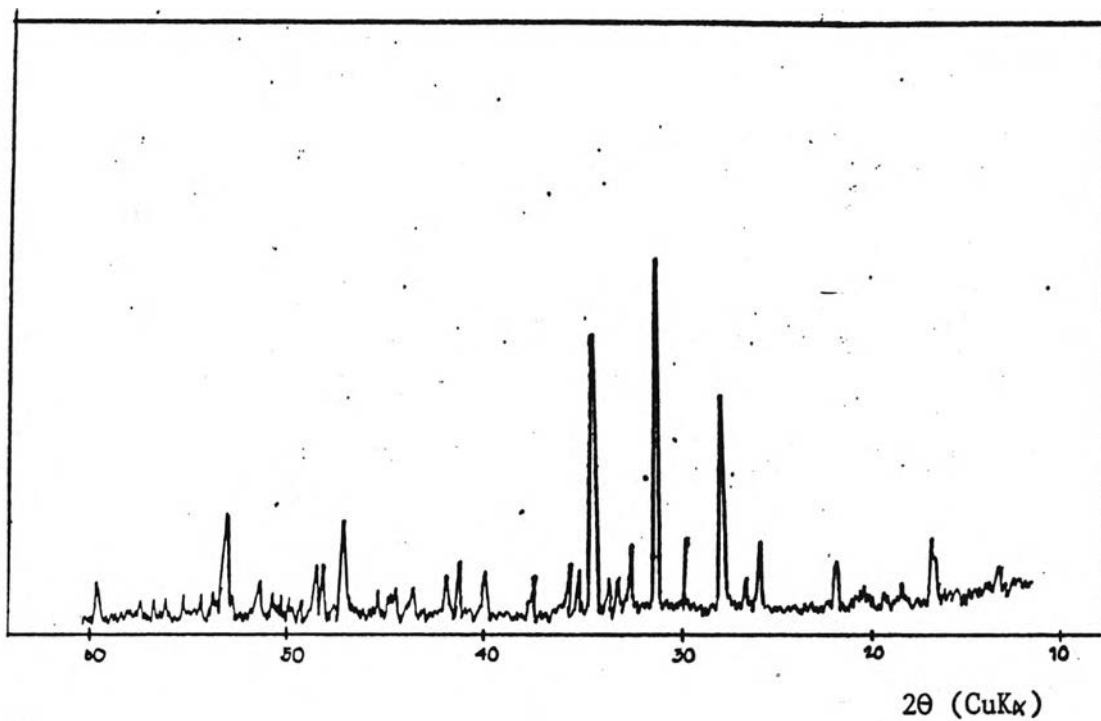
2θ (CuKα)



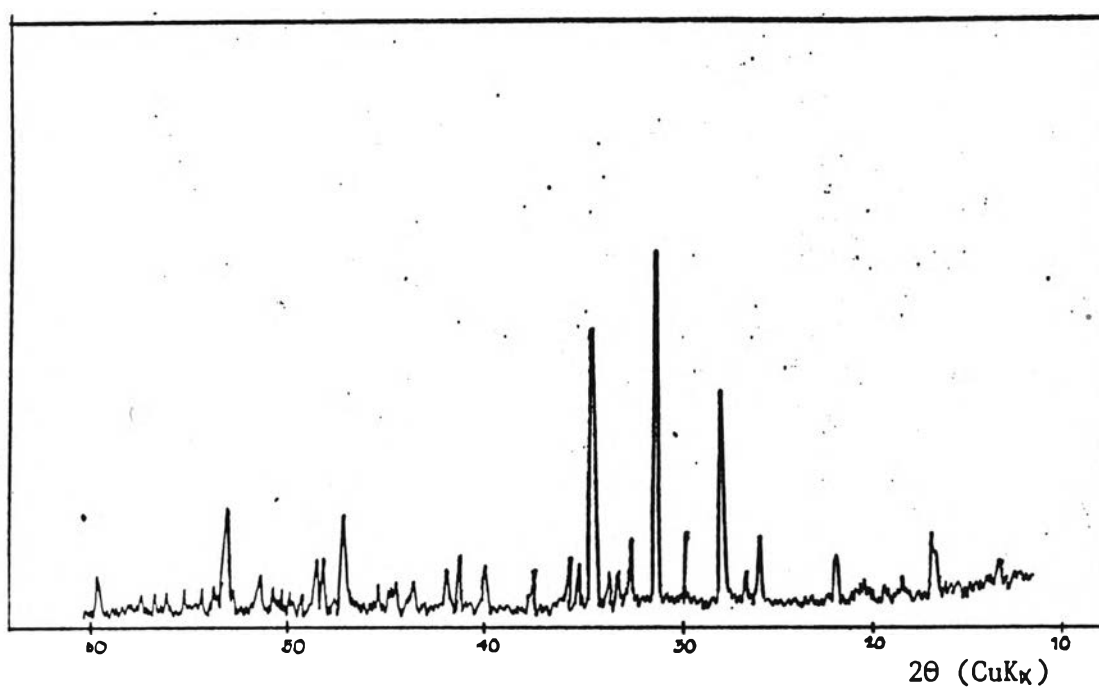
(b)

2θ (CuKα)

Fig. 27 X-ray diffraction patterns of prepared DCPD stoichiometrically mixed with calcium carbonate heated at 1100 C. 3 hours with and without quenching in air (a) Fast cooling (b) Slow cooling.

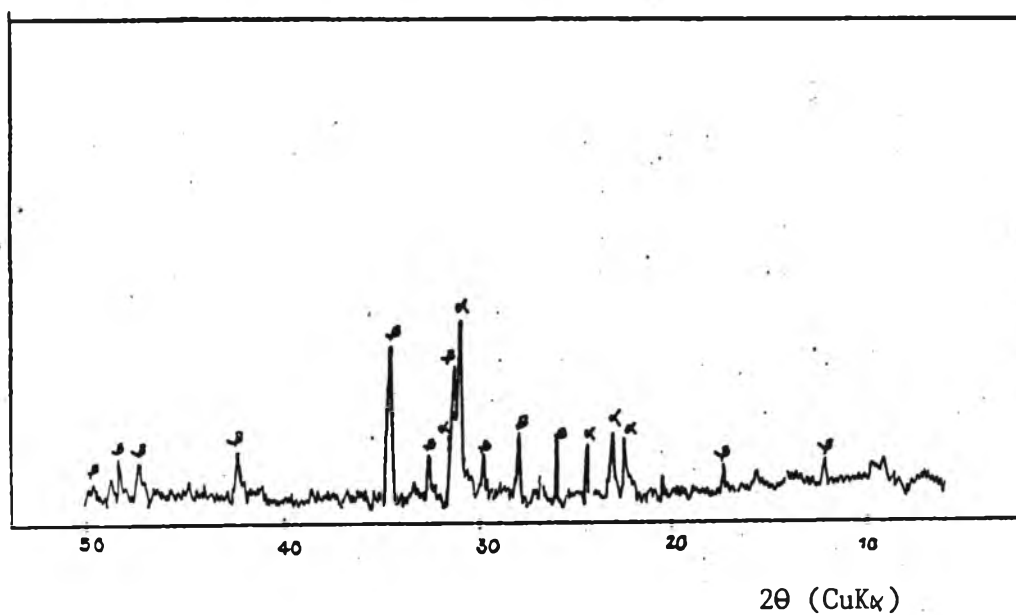


(a)

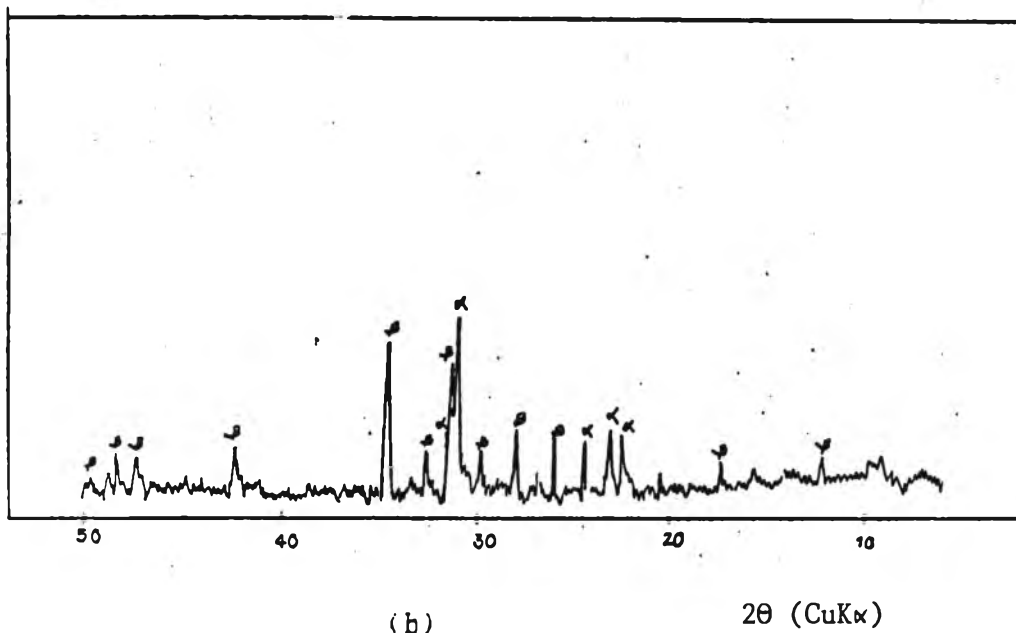


(b)

Fig. 28 X-ray diffraction patterns of reference DCPD stoichiometrically mixed with calcium carbonate heated at 1100°C . 3 hours with and without quenching in air (a) Fast cooling (b) Slow cooling.

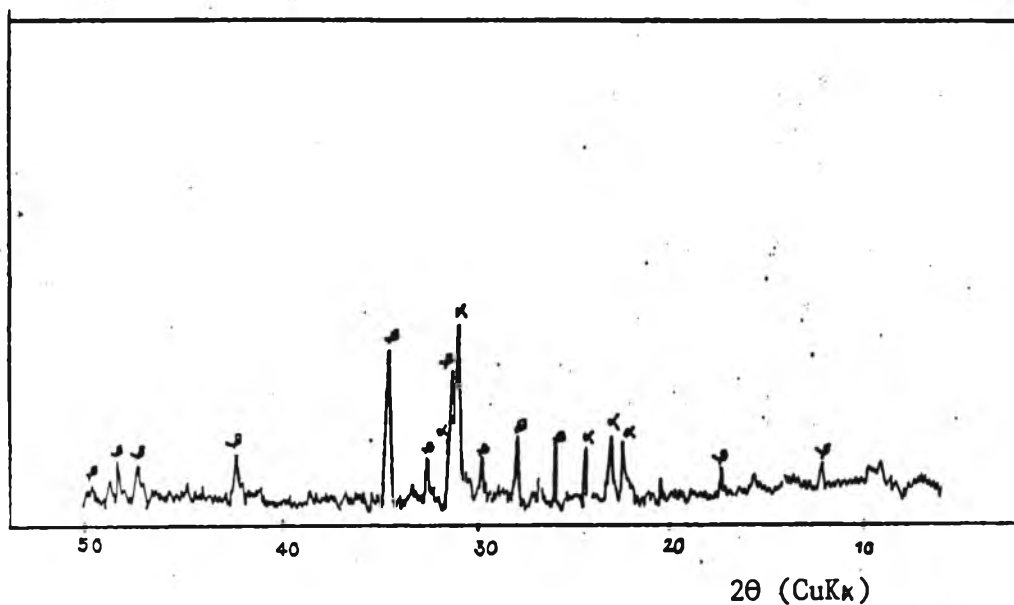


(a)

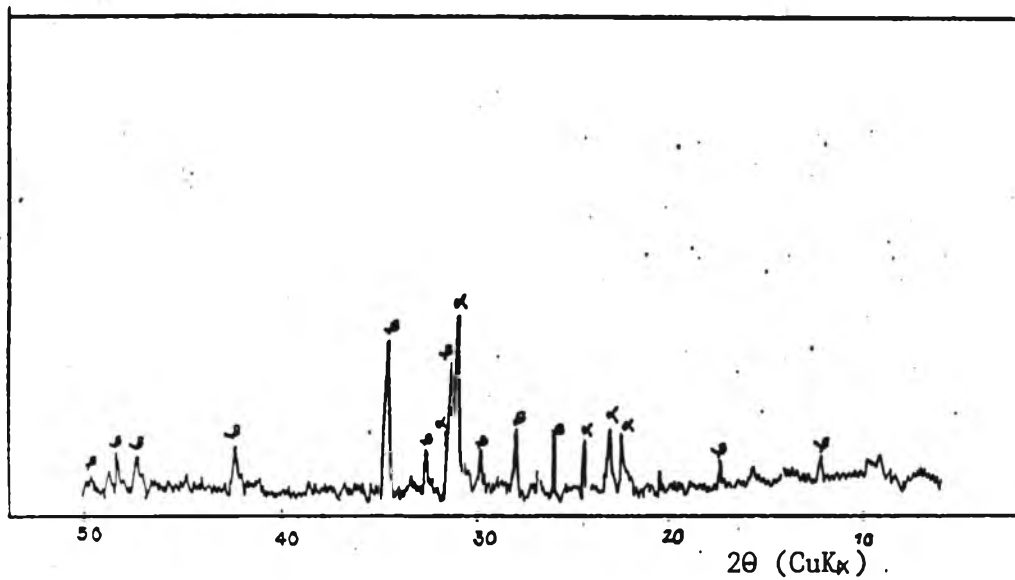


(b)

Fig. 29 X-ray diffraction patterns of prepared DCPD stoichiometrically mixed with calcium carbonate heated at 1200 C. 3 hours with and without quenching in air (a) Fast cooling (b) Slow cooling.

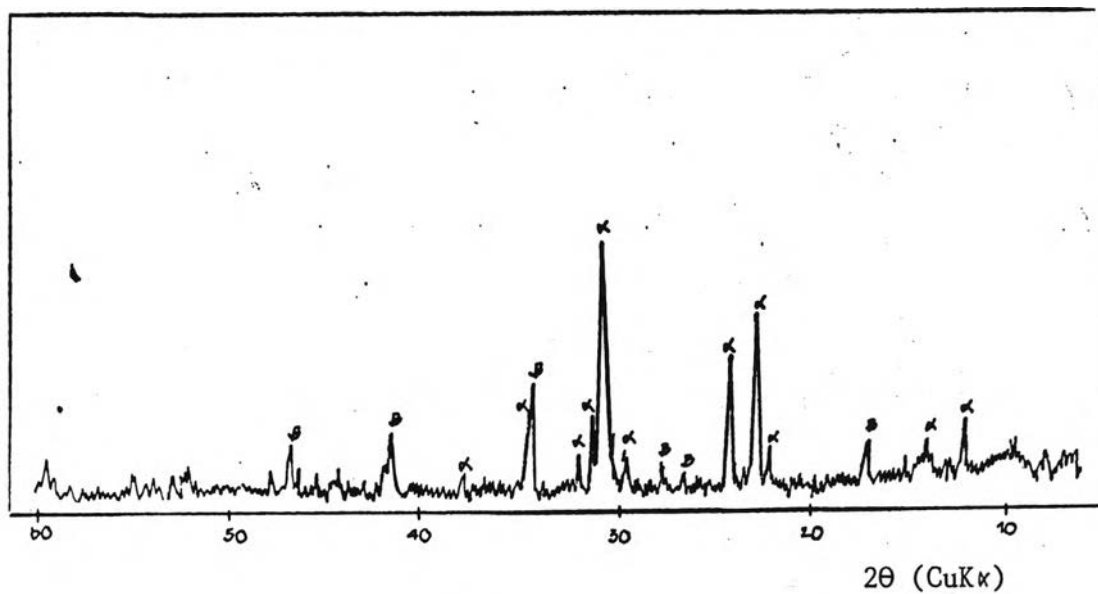


(a)

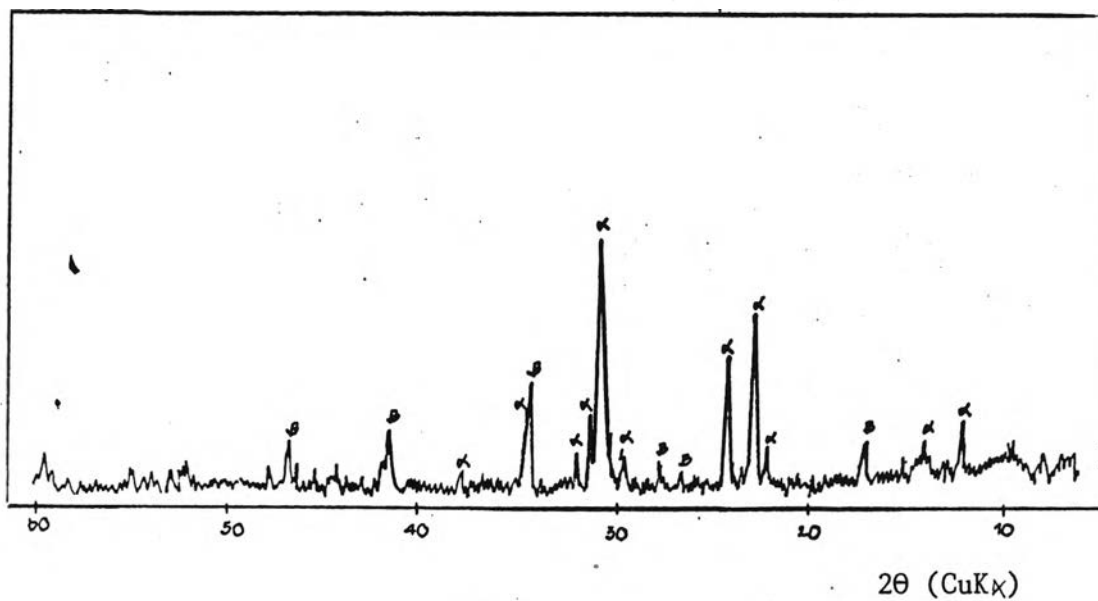


(b)

Fig. 30 X-ray diffraction patterns of reference DCPD stoichiometrically mixed with calcium carbonate heated at 1200°C, 3 hours with and without quenching in air (a) Fast cooling (b) Slow cooling.



(a)



(b)

Fig. 31 X-ray diffraction patterns of prepared DCPD stoichiometrically mixed with calcium carbonate heated at 1300°C, 3 hours with and without quenching in air (a) Fast cooling (b) Slow cooling.

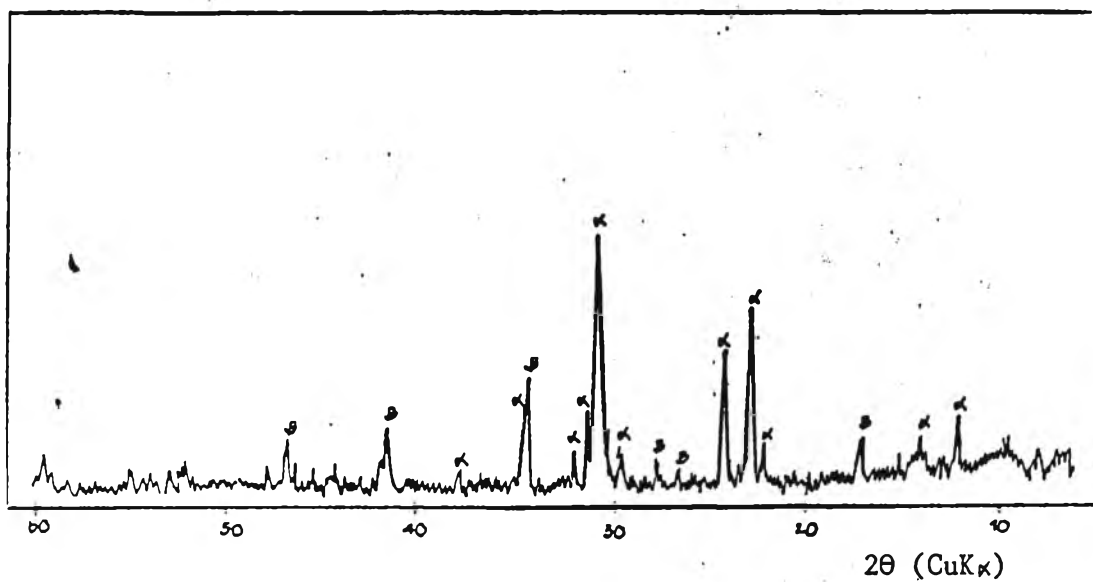
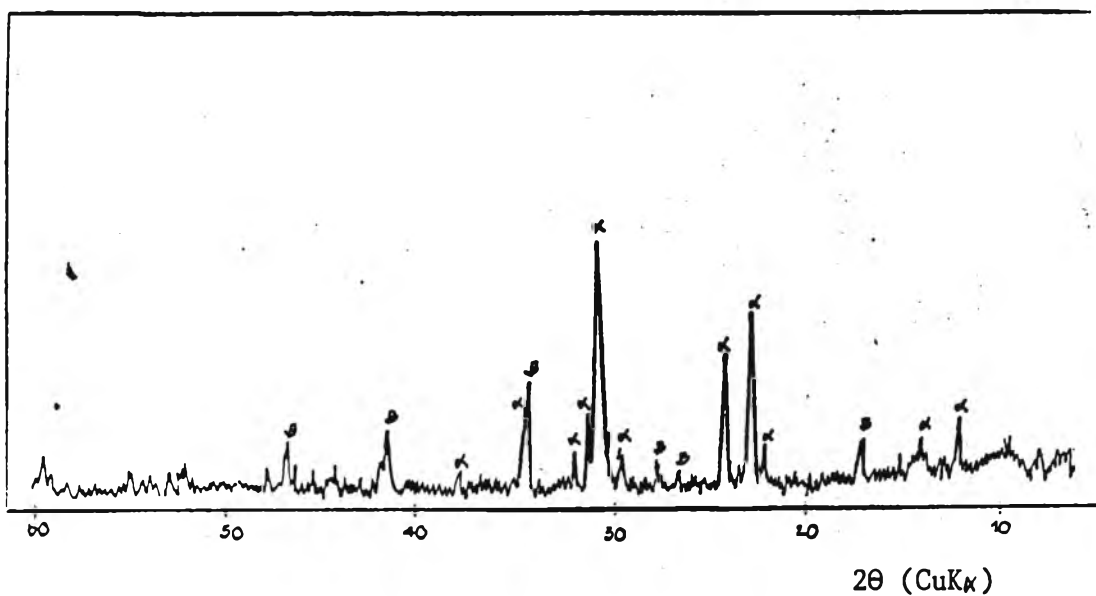


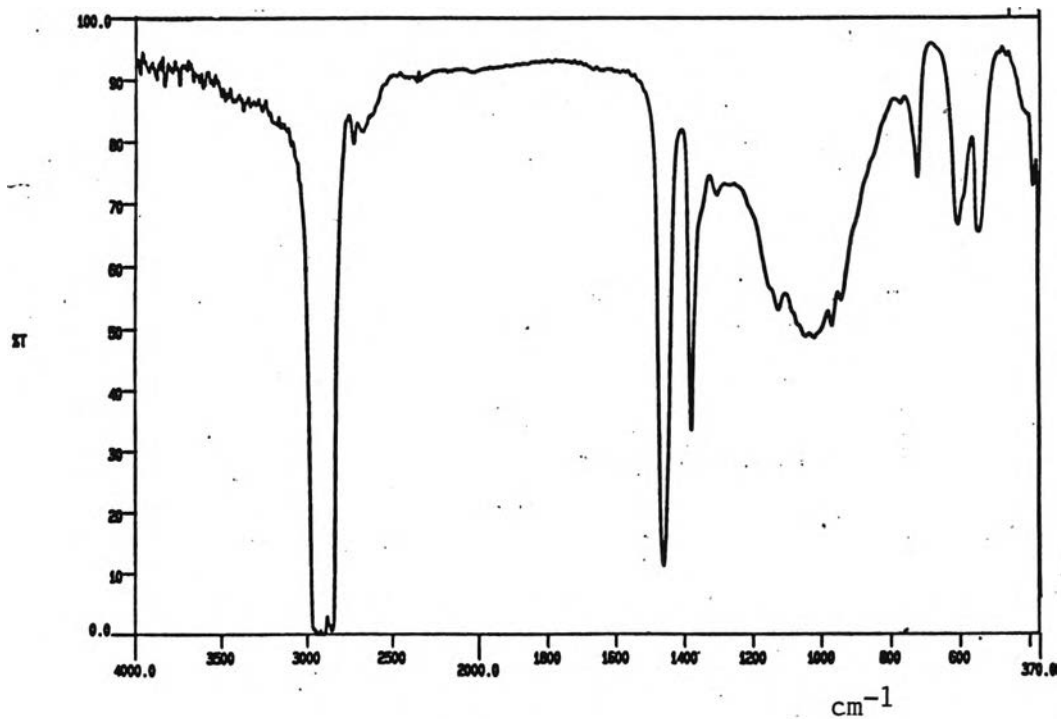
Fig.32 X-ray diffraction patterns of reference DCPD stoichiometrically mixed with calcium carbonate heated at 1300°C .3 hours with and without quenching in air. (a) Fast cooling (b) Slow cooling.



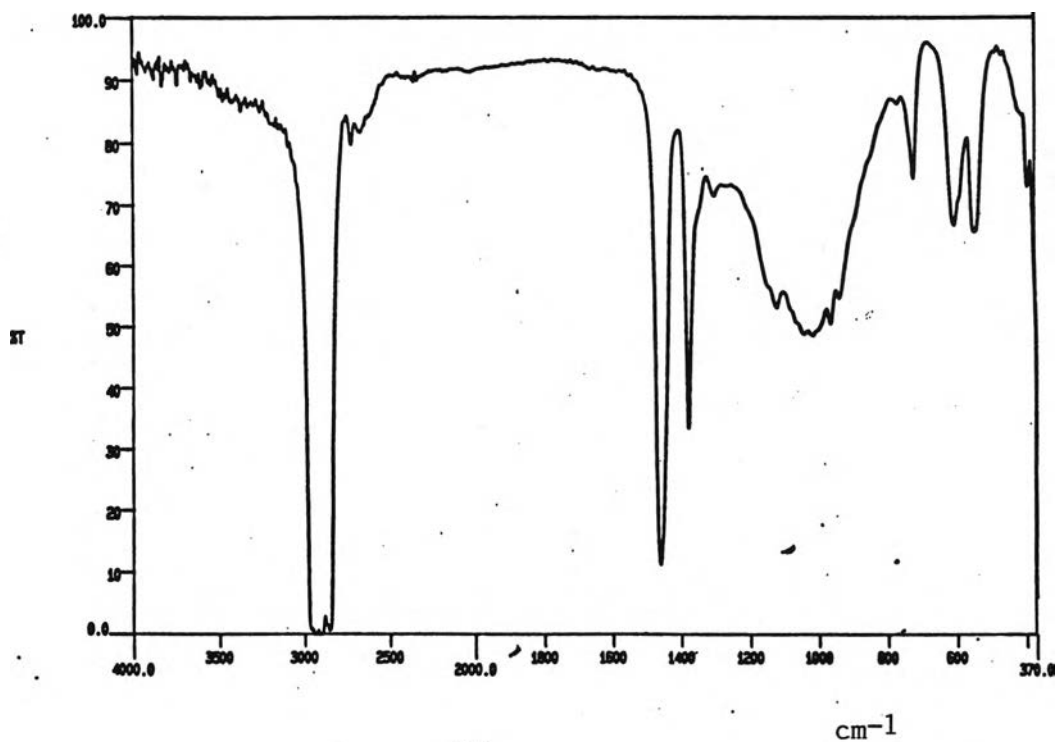
### 4.3.3 Infrared Spectra

The IR spectra of the prepared DCPD stoichiometrically mixed with calcium carbonate heated at 1100, 1200 and 1300 °C, 3 hours fast and slow cooling, from wavenumber 4000 to 370  $\text{cm}^{-1}$  using the Nujol mull technique were shown in Fig. 37:a,b ; 38:a,b ; 39:a,b.

The detected bands attributed to the  $\text{PO}_4^{3-}$  in  $\beta$ -TCP and  $\alpha$ -TCP at wavelenght 1110-970  $\text{cm}^{-1}$ . From the results in Fig. 31-39, and the Table 13, the identification of TCP phase was confirmed and summarized in Table 14.



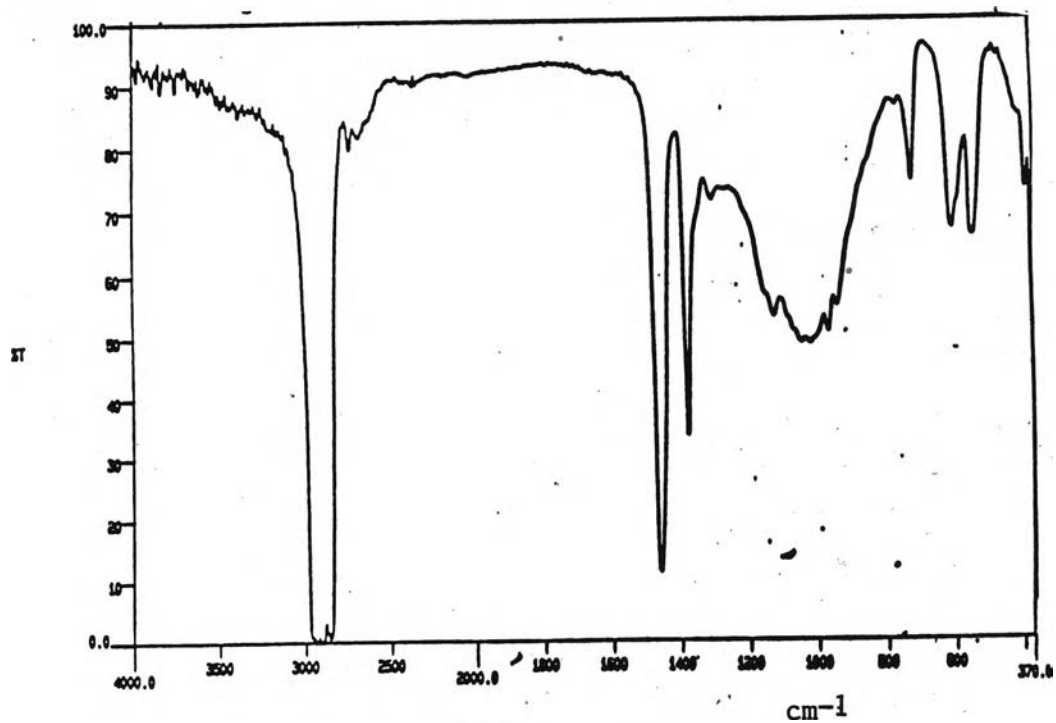
(a)



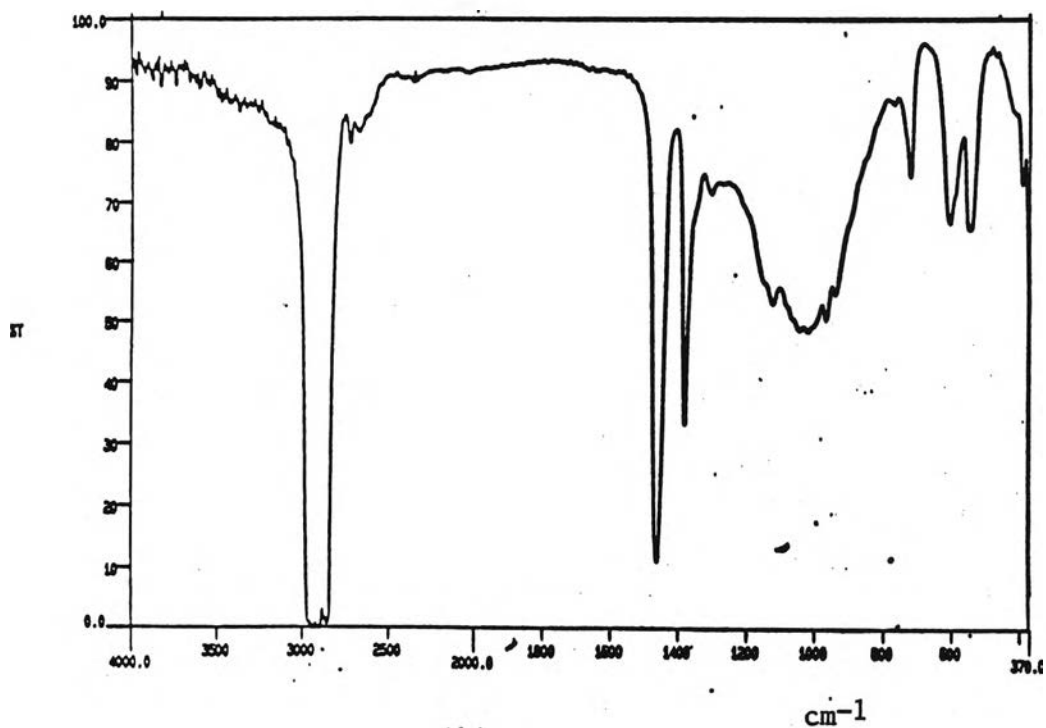
(b)

Fig. 33 IR spectra of prepared DCPD stoichiometrically mixed with calcium carbonate heated at 1100°C, 3h. with and without quenching in air

(a) Fast cooling (b) Slow cooling.



(a)



(b)

Fig. 34 IR spectra of prepared DCPD stoichiometrically mixed with calcium carbonate heated at 1200°C, 3 h. with and without quenching in air

(a) Fast cooling (b) Slow cooling.

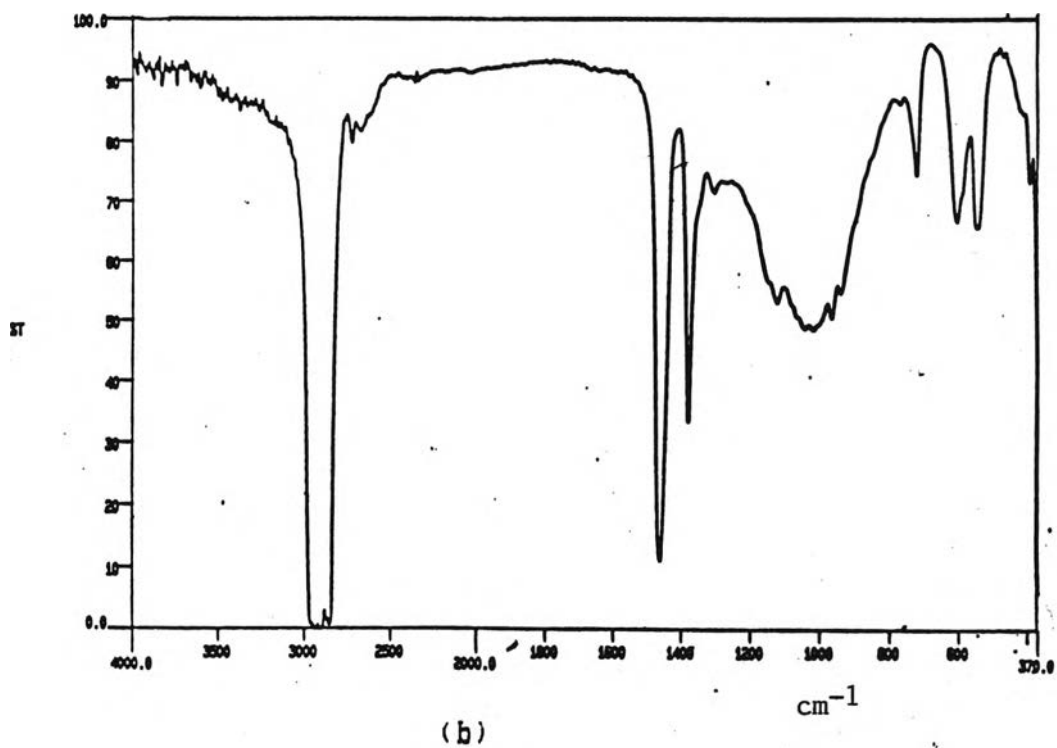
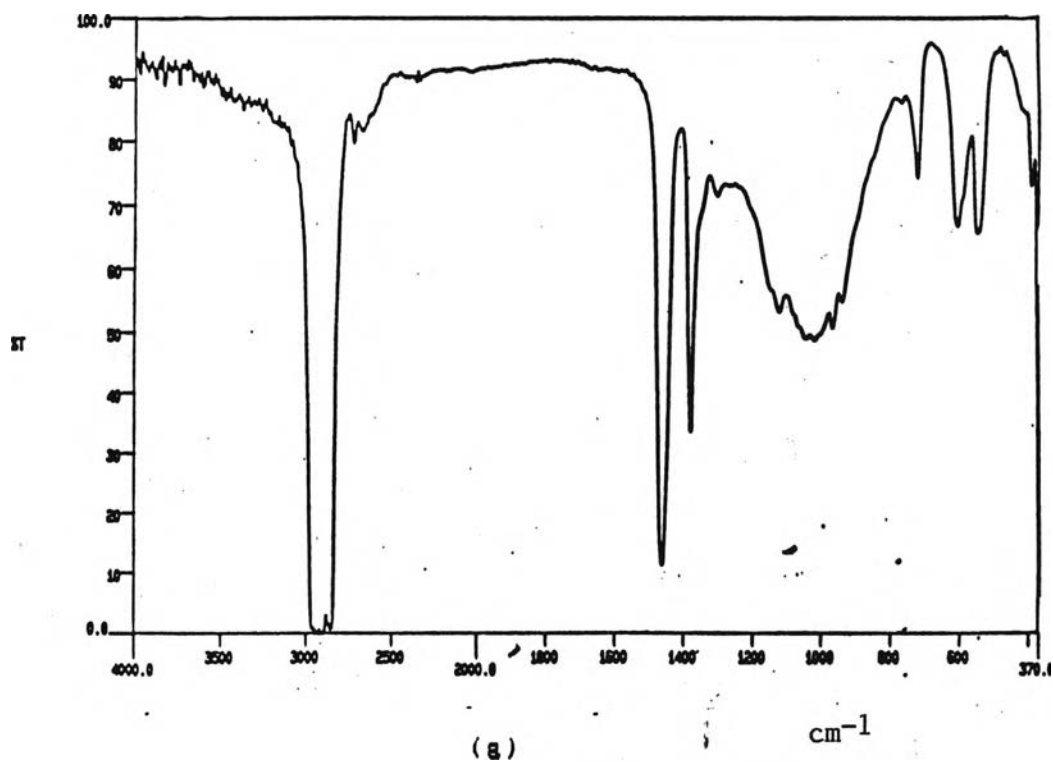


Fig. 35 IR spectra of prepared DCPD stoichiometrically mixed with calcium carbonate heated at 1300°C .3 h. with and without quenching in air

(a) Fast cooling      (b) Slow cooling.

## 4.3.4 Ca/P mole ratio.

Table 14 Ca/P mole ratio of prepared TCP from prepared DCPD stiochiometrically mixed with calcium carbonate heated at various temperatures by fast and slow cooling techniques , characterized by Mineral Assay and Service.

Heat Treatment °C / hours	Fast-cooled Technique	Slow-cooled Technique
1100°C / 3	1.47	1.46
1300°C / 3	1.51	1.50

The value of Ca/P mole ratio obtained in Table 13 are all close to 1.5 which correspond to that of TCP .

From the results in Fig.27-35 and Table 13 , the identification of TCP phase was confirmed and summarized in Table 15

Table 15 Identification of products from prepared and standard DCPD stoichiometrically mixed with calcium carbonate heated at various temperature by fast and slow cooling techniques.

Type of Sample	Heat-Treatment °C/hours	Fast-cooled Sample	Slow-Cooled Sample
Prepared DCPD			
+CaCO <sub>3</sub>	1100/3	β-TCP	β-TCP
	1200/3	β-TCP+α-TCP	β-TCP+α-TCP
	1300/3	α-TCP+β-TCP	α-TCP+β-TCP
reference DCPD			
+CaCO <sub>3</sub>	1100/3	β-TCP	β-TCP
	1200/3	β-TCP+α-TCP	β-TCP+α-TCP
	1300/3	α-TCP+β-TCP	α-TCP+β-TCP

\* First phase listed is the more dominant phase in the heated material.

The results of experiments indicated that  $\beta$ -TCP was the only product received from the prepared DCPD as well as from the reference DCPD when stoichiometrically mixed with calcium carbonate and heated at 1100°C for 3 hours. Upon treatment at and 1200°C for 3 hours, however  $\beta$ -TCP partly transformed to  $\alpha$ -TCP. The quantity of  $\alpha$ -TCP increased with temperature up to 1300°C. There was no difference between a slowly cooled and air quenched products.

According to the phase diagram shown in Fig. 36 CaO-2CaO.P<sub>2</sub>O<sub>5</sub> system (Welch and Gutt, 1961); at 1125°C,  $\beta$ -TCP transforms to  $\alpha$ -TCP at 1125°C already, but the product is not pure (solid solution of  $\alpha$ -TCP). This corresponded to the results of this experiment in which the sample heated at 1200°C for 3 hours.  $\beta$ -TCP partly transformed to  $\alpha$ -TCP only partially. But it contradicts to the phase diagram as shown in Fig.37 (Hill et al, 1994) ;according to the latter phase diagram, the product at approximately 1200°C is a mixture between  $\beta$ -Ca<sub>3</sub>PO<sub>4</sub> and  $\alpha$ -Ca<sub>2</sub>P<sub>2</sub>O<sub>7</sub>.

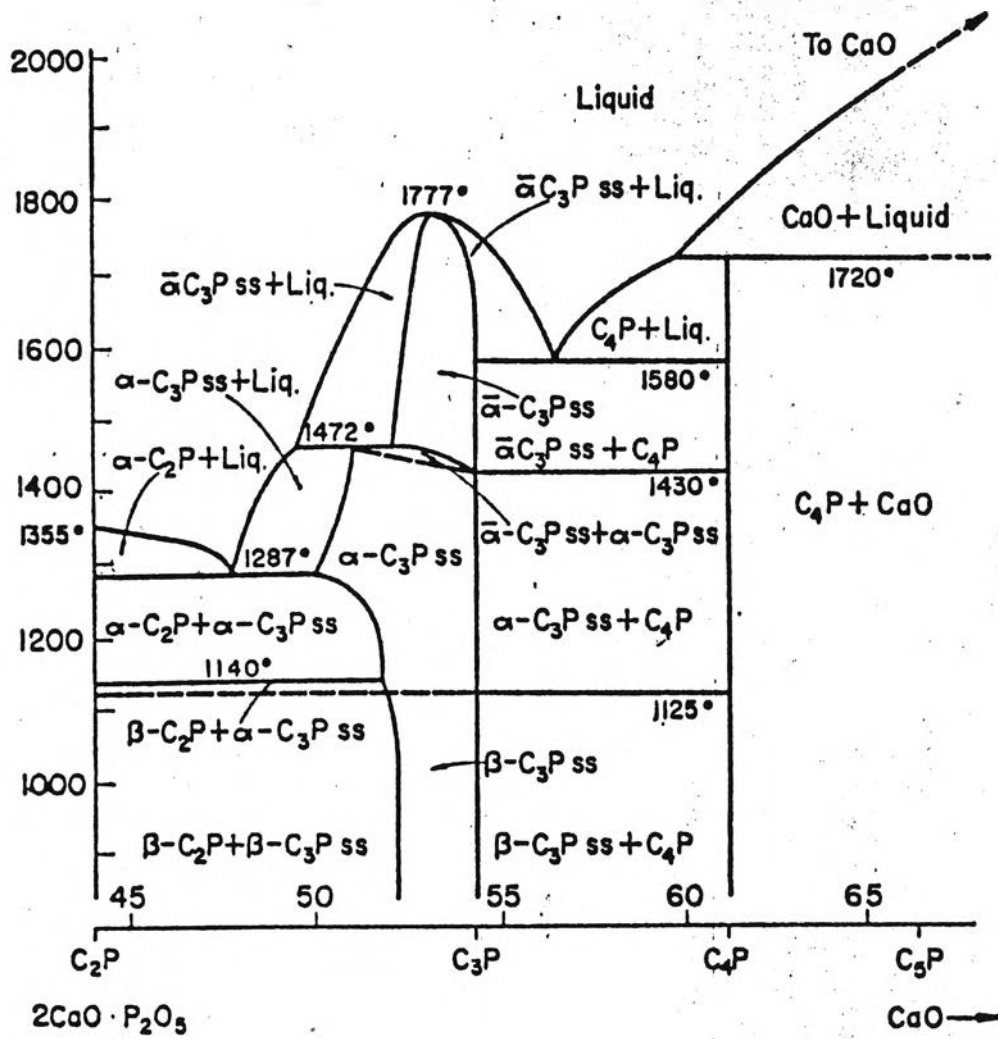
CaO-P<sub>2</sub>O<sub>5</sub>

Fig.36 Phase diagram, system CaO-2CaO.P<sub>2</sub>O<sub>5</sub>.

C = CaO, P = P<sub>2</sub>O<sub>5</sub>. (Welch and Gutt, 1961)



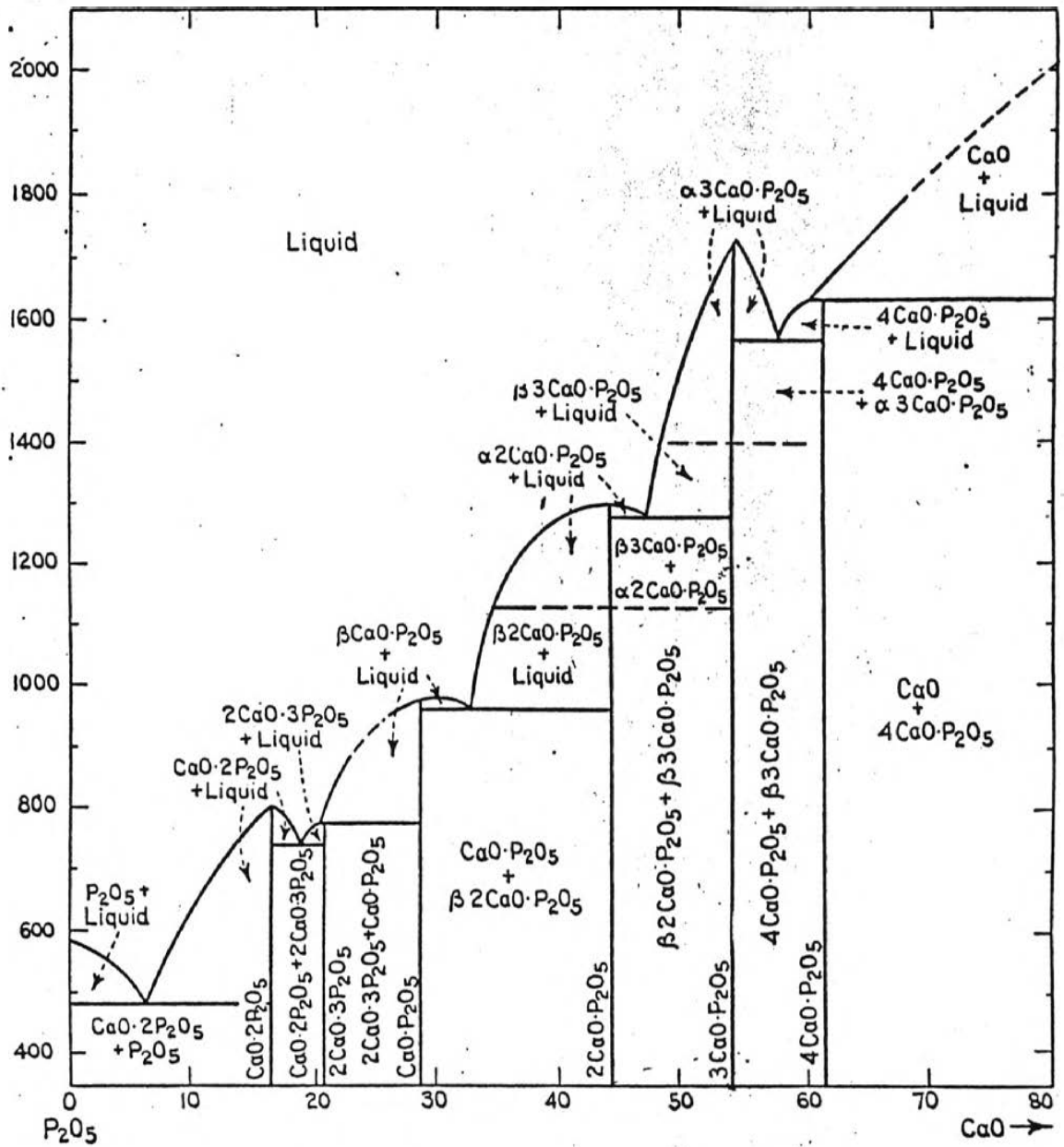
$\text{CaO}-\text{P}_2\text{O}_5$ 


Fig.37 Phase diagram , system  $\text{CaO}-\text{P}_2\text{O}_5$ .

(Hill et.al, 1994)